Chemical Engineering Science 104 (2013) 908–924

Contents lists available at ScienceDirect

Chemical Engineering Science

journal homepage: www.elsevier.com/locate/ces

Review

Membranes from nanoporous 1D and 2D materials: A review of opportunities, developments, and challenges

Wun-gwi Kim, Sankar Nair*

School of Chemical & Biomolecular Engineering, Georgia Institute of Technology, Atlanta, GA 30332-0100, USA

ARTICLE INFO

Article history:
Received 20 July 2013
Received in revised form
21 September 2013
Accepted 24 September 2013
Available online 16 October 2013

Keywords:
Membranes
Layered materials
Nanoporous
Nanotubes
Separations
Nanocomposites

ABSTRACT

Membranes utilizing nanoporous one-dimensional (1D) and two-dimensional (2D) materials are emerging as attractive candidates for applications in molecular separations and related areas. Such nanotubular and nanolayered materials include carbon nanotubes, metal oxide nanotubes, layered zeolites, porous layered oxides, layered aluminophosphates, and porous graphenes. By virtue of their unique shape, size, and structure, they possess transport properties that are advantageous for membrane and thin film applications. These materials also have very different chemistry from more conventional porous 3D materials, due to the existence of a large, chemically active, external surface area. This feature also necessitates the development of innovative strategies to process these materials into membranes and thin films with high performance. This work provides the first comprehensive review of this emerging area. We first discuss approaches for the synthesis and structural characterization of nanoporous 1D and 2D materials. Thereafter, we elucidate different approaches for fabrication of membranes and thin films from these materials, either as multiphase (composite/hybrid) or single-phase membranes. The influence of surface chemistry and processing techniques on the membrane morphology is highlighted. We then discuss the applications of such membranes in areas relating to molecular transport and separation, *e.g.* gas and liquid-phase separations, water purification, and ion-conducting membranes. The review concludes with a discussion of the present outlook and some of the key scientific challenges to be addressed on the path to industrially applicable membranes containing nanoporous 1D and 2D materials.

Contents

1. Introduction . . . 909
   1.1. Polymeric and inorganic membranes . . . 909
   1.2. Composite ('mixed matrix') membranes . . . 910
   1.3. Membranes incorporating 1D and 2D materials . . . 910
2. Membrane-Forming 1D and 2D materials . . . 910
   2.1. Nanotubular (1D) materials . . . 910
   2.2. Layered oxide (2D) materials . . . 911
      2.2.1. MCM-22, ITQ, and Nu-6 . . . 912
      2.2.2. AMH-3 . . . 912
      2.2.3. Layered MFI . . . 913
      2.2.4. Layered titanosilicates and aluminophosphates . . . 913
   2.3. Graphene-based materials . . . 913
3. Processing of membranes containing 1D and 2D materials . . . 915
   3.1. Nanocomposite membranes . . . 915
      3.1.1. Composite membranes with nanotubes . . . 915
      3.1.2. Composite membranes with porous layered oxides . . . 915
   3.2. All-inorganic membranes . . . 916
   3.3. Microstructural analysis of nanocomposite membranes . . . 917

* Corresponding author. Tel.: +1 4048 944 826.
E-mail address: sankar.nair@chbe.gatech.edu (S. Nair).

0009-2509/$ - see front matter © 2013 Elsevier Ltd. All rights reserved.
http://dx.doi.org/10.1016/j.ces.2013.09.047

4. Separation applications . . . 918
4.1. 1D nanotubular membranes . . . 918
4.2. 2D layered oxide membranes . . . 919
4.3. Graphene and other carbon membranes . . . 921
5. Outlook and challenges . . . 921
Acknowledgment . . . 922
References . . . 922

1. Introduction

Advanced membrane separations have generated much interest in the last two decades, owing to their potential for technological impact in the energy, fuels, petrochemical, and renewable chemical sectors (Pandey and Chauhan, 2001; Vane, 2005; Jagur-Grodzinski, 2007; Bernardo et al., 2009). Conventional separation methods, currently in heavy use for petrochemical processing, are increasingly challenged by energy cost, performance limitations, and environmental (*e.g.*, carbon) footprint. Other important technological problems such as large-scale potable water production, greenhouse gas capture, and production of renewable fuels and chemicals, also require energy-efficient, environmentally benign, and lower-cost separation technologies that are unlikely to be dominated by conventional processes such as distillation, liquid absorption and stripping, crystallization, and liquid extraction. At the same time, the science and technology of membrane fabrication and scale-up has made considerable progress over the last decade, further brightening the prospects for future large-scale commercial applications replacing conventional separations processes.

Polymeric and inorganic membranes have received substantial research and development attention (as summarized in the following section), but are constrained by trade-offs in performance metrics or by lack of scalability of processing techniques. Nanocomposite/hybrid membranes, which typically contain a high-performance inorganic materials (fillers) dispersed in a polymeric matrix, have gained ground as a means of combining the best characteristics of polymeric and inorganic materials while potentially overcoming their individual limitations. Most nanocomposite membranes contain fillers of isotropic or near-isotropic morphologies, with dimensions typically in the 100–1000 nm range. However, it has been realized for some time that membranes containing strongly anisotropic and low-dimensional fillers would offer some unique possibilities and advantages. These possibilities have moved closer to realization in the last decade, owing to key breakthroughs in the synthesis and characterization of anisotropic and low-dimensional separation materials and their fabrication into functional membranes by different processing strategies.

This review focuses on understanding the current state of the art, opportunities, and challenges in the science and engineering of membranes containing one-dimensional (1D) and two-dimensional (2D) nanoscopic materials. The 1D materials considered are primarily of nanotubular structure, and it is desired to obtain fast, selective permeation of molecules through their tubular nanopores. For membrane transport applications, a perpendicular (*i.e.*, transmembrane) orientation of the 1D materials embedded in the membrane is expected to be strongly preferable over random or in-plane orientations. The 2D materials of interest are primarily those with a layer-like morphology characterized by a high aspect ratio (large lateral dimensions and small thickness), and containing nanoporous 'perforations' spanning the layer thickness through which selective molecular transport can occur. In this introductory section, we overview the state of polymeric, inorganic, and isotropic composite membranes, and contrast these membrane morphologies with emerging membrane architectures containing 1D and 2D materials. In the subsequent sections, we present an overview of the main classes of 1D and 2D materials synthesized for use in membranes, and discuss the processing routes that have been developed for fabricating membranes comprising these materials. We then review the characterization and separation performance of such membranes, and conclude with a discussion of the current challenges and prospects in this area.

1.1. Polymeric and inorganic membranes

Polymers used for fabricating membranes can be semi-crystalline (*e.g.*, polyvinylalcohol and cellulose acetate), glassy (*e.g.*, polysulfone and polyimides), or elastomeric (*e.g.*, silicone-based polymers). These polymers show a variety of structural and dynamical behavior, leading to a large range of molecular permeation properties. While diffusivity and solubility both determine the *permeability* of molecules in polymers, the *selectivity* of glassy polymers for one kind of molecule over another is mainly governed by diffusivity differences. Glassy polymers mainly exploit size exclusion effects arising from differences in the kinetic diameters of molecules (Stern et al., 1989; Park and Paul, 1997). However, selectivity in elastomers is dominated by solubility differences, and hence more condensible large molecules (such as hydrocarbons) are more permeable in elastomers than small gases like N_2. Elastomeric polymer membranes can be used to separate organic vapors from non-condensible gases such as air (Schultz and Peinemann, 1996; Pinnau and He, 2004). This behavior is sometimes referred to as 'reverse selectivity' in relation to the properties of glassy polymers. Semicrystalline and glassy polymers find commercial applications in natural gas purification and dehydration of organic/water mixtures. However, the largest obstacle in utilization of polymeric membranes in industrial applications is their intrinsic trade-off relationship between selectivity and permeability, embodied in the Robeson plot (Robeson, 2008).

Nanoporous inorganic materials offer much higher permeabilities than polymers, and also high selectivities in many separations of technological interest. Nanoporous materials such as zeolites and metal-organic frameworks (MOFs) can be fabricated into selective separation membranes that exploit their molecular-sieving nanopores (Davis, 2002; Snyder and Tsapatsis, 2007; Shah et al., 2012). Membranes of various zeolites such as MFI, FAU and LTA are being developed for separation applications (Caro and Noack, 2008). Despite two decades of development on zeolite membranes, and a few commercialized applications such as alcohol dehydration, zeolite membranes are presently not widely utilized due to the difficulties their economical and quality-controlled fabrication on a large scale. Challenging issues in zeolite membranes, such as reproducibility of membrane manufacture and control over defect formation must be overcome to realize the industrial applications of zeolite membranes (Choi et al., 2009a; Gascon et al., 2012).

1.2. Composite ('mixed matrix') membranes

'Mixed matrix' membranes (MMMs) can be prepared by incorporating appropriately chosen inorganic particles in a polymeric matrix. In doing so, it is hoped (Koros, 2004) that MMMs can combine the advantages of polymers (such as good processibility, scalable fabrication, and lower cost) with those of inorganic materials (such as high permeability, selectivity, and thermal/mechanical stability). Many research groups have incorporated various inorganic materials such as zeolites, MOFs, and other molecular sieves into polymer matrices. Some pioneering works on this topic include the incorporation of zeolite 4A in the polyimide Matrimid (Mahajan and Koros, 2002), carbon molecular sieves in Matrimid (Vu et al., 2003), fumed-silica nanoparticles in poly(4-methyl-2-pentyne) (Merkel et al., 2002), zeolite MFI or carbon black materials in PDMS (Moermans et al., 2000; Vane et al., 2008). A large number of works have followed these early reports, and have been recently reviewed (Nasir et al., 2013). An important theme in mixed matrix membranes is the improvement of interfacial compatibility between the polymer matrix and the filler particles. For example, in the case of zeolite materials a number of surface-treatment methodologies have been developed to improve interfacial adhesion and filler dispersion, thereby leading to higher separation performance (Shu et al., 2007; Bae et al., 2009). MMMs incorporating MOF materials have also been reported in the recent literature, and are reviewed elsewhere (Jeazet et al., 2012). Overall, MMMs are making their way to reaching performance levels viable for technological consideration over polymeric membranes. The problem of scalable processing of MMMs is non-trivial, but perhaps less difficult than the processing of zeolitic membranes. Specifically, the physics of transport in MMMs dictates that high filler loadings (30–50 wt%) are usually required to obtain substantial improvements over the base polymeric membrane (Adams et al., 2011). The scalable fabrication of thin (submicron) MMMs containing large filler fractions (Pendergast and Hoek, 2011) is challenging and is a topic of ongoing work. Furthermore, the study of transport phenomena in MMMs also reveals an intrinsic limitation of using isotropic fillers, namely the high probability of permeating molecules bypassing the filler particles (Vinh-Thang and Kaliaguine, 2013).

1.3. Membranes incorporating 1D and 2D materials

Porous 1D nanotubular (Cong et al., 2007; Ismail et al., 2009; Kang et al., 2012) and 2D layered (Jeong et al., 2004; Galve et al., 2011, Zornoza et al., 2011) materials have been suggested as leading to membranes with unique transport properties, that could overcome the limitations of isotropic inorganic fillers in MMMs. Fig. 1 illustrates the structures of idealized membranes containing 1D and 2D materials. In Fig. 1a, the nanotube materials are shown as vertically aligned and completely spanning the thickness of the membrane. By realizing such an ideal structure through an appropriate fabrication process, favorable properties of nanotubes such as fast molecular transport can be most efficiently exploited. The potentially tunable functionality of the nanotube mouths, as well as inner and outer surfaces, can be used to expand the range of separations applications and compatibility with various types of matrix materials. Fig. 1b shows a schematic diagram of a membrane incorporating high-aspect ratio layered (2D) materials. In comparison to isotropic fillers, the high aspect ratio of the layers or 'flakes' necessitate longer and more tortuous paths for the larger molecule that cannot easily pass through the pores, and thereby effectively decrease the permeability of the larger molecule (Ray and Okamoto, 2003). At the same time, the nanoscopic thickness of the flakes allows fast permeation of the smaller molecule. For the above reasons, it is hypothesized that membranes containing nanoscopically thin flakes can allow high separation performance with a much lower loading of the flakes than required for isotropic fillers. From the viewpoint of membrane fabrication and scale-up, the nanoscopically thin layered flakes are favorable because they can be incorporated in ultra-thin membranes such as the skin layers of hollow fiber membranes (Johnson and Koros, 2009). Beyond their utilization in composite membranes, 2D materials could also be used to form purely inorganic membranes. Direct deposition or coating of the flakes on porous supports could provide a less challenging alternative to fabrication of inorganic membranes by hydrothermal growth on the support.

2. Membrane-Forming 1D and 2D materials

2.1. Nanotubular (1D) materials

Fig. 2a shows the molecular structure of a single-walled carbon nanotube (SWNT) and a multi-walled carbon nanotube (MWNT) (Ismail, 2011). These nanotubes are based upon the graphitic sheet structure of hexagonally arranged carbon atoms with sp_2 hybridization. This arrangement contributes to the unique mechanical and electronic properties of carbon nanotubes (CNTs), which are under intense investigation for a variety of applications. CNTs have been used to form composites with polymers, specifically for mechanical reinforcement and improvement in electrical conductivity (Roy et al., 2012; Tkalya et al., 2012). The hollow tubular morphology of the CNT has also led to its suggestion as a permeable and mechanically strong filler material for membrane-based molecular separations (Goh et al., 2013). A primary advantage of CNTs as membrane materials is the very high flux that can be obtained, due to the atomically smooth nature of the walls. However, the corresponding drawback is a lack of high selectivity for different molecules through a pristine CNT (Kim et al., 2007). The electronic structure of the inner wall of the CNT is considered essentially unreactive and difficult to functionalize with organic or other moieties that may impart selectivity (Chamberlain et al., 2011) Another key challenge for CNT-based membrane materials is the

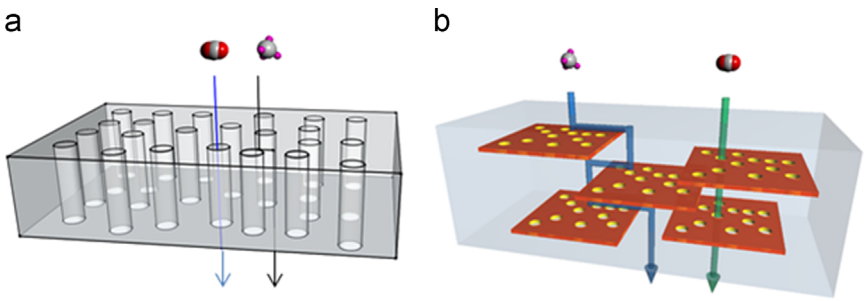

Fig. 1. Schematic diagrams of composite membranes incorporating (a) 1D nanotubular materials, and (b) 2-D nanoplatelets (adapted from Kim et al., 2013).

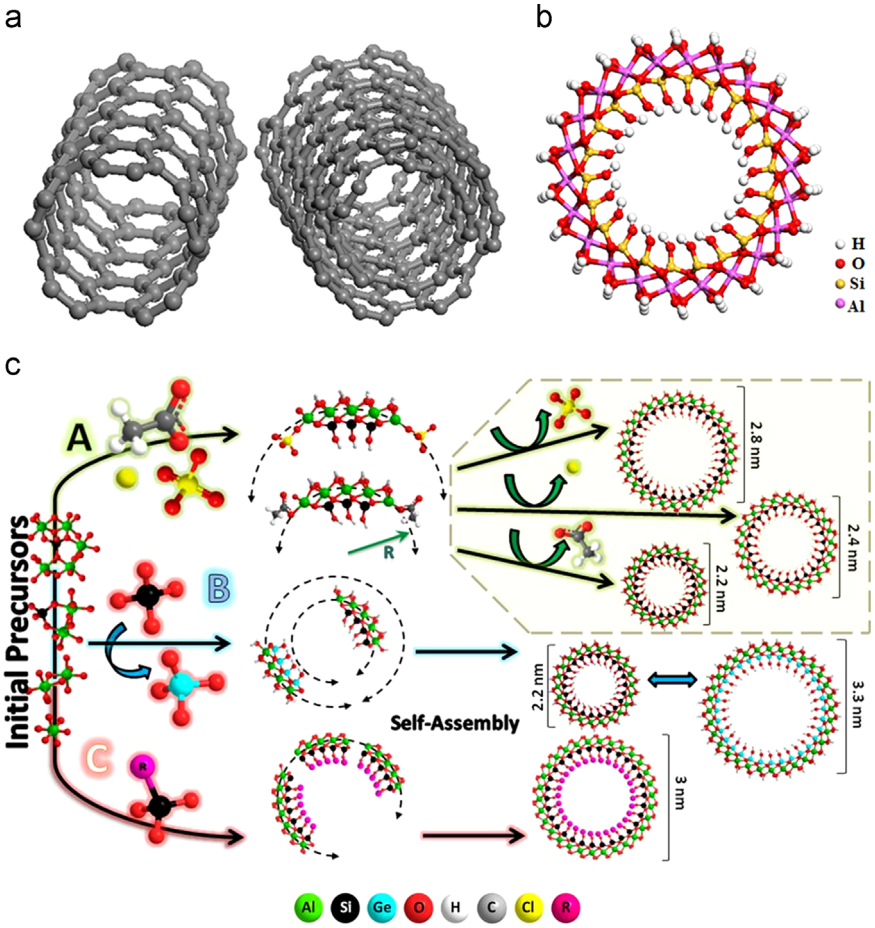

Fig. 2. Structures of (a) single- and multi-walled carbon nanotubes (SWNTs/MWNTs), (b) a single-walled aluminosilicate nanotube, and (c) summary of molecular-level approaches to control the curvature and composition of single-walled metal oxide nanotubes (adapted from Yucelen et al., 2012).

unsatisfactory interface compatibility between CNTs and many membrane-forming polymers, which results in defect formation in CNT/polymer nanocomposite membranes (Ismail et al., 2009). Several routes for modification of the outer surface of CNTs are available, including covalent and non-covalent binding with desired substituents (Vaisman et al., 2006; Zhao and Stoddart, 2009).

Inorganic nanotubes, in the form of metal oxides, have several advantages over CNTs for membrane applications (Mukherjee et al., 2007; Rao and Govindaraj, 2009; Tenne and Seifert, 2009). A wide range of multi-walled inorganic nanotubes with large pore diameters in the 10–50 nm range have been synthesized (Tenne and Seifert, 2009); however, single-walled (or few-walled) nanotubes with pore diameters in the ~1 nm or sub-nm range are clearly much more suitable for molecular separations. Although the currently available repertoire of such materials is not large, several interesting materials of this type are known. These include single-walled aluminosilicate or aluminogermanate-based nanotubes which are synthetic analogs of the nanotube mineral imogolite. The structure of the single-walled aluminosilicate nanotube is illustrated in Fig. 2b. The outer wall is composed of a hexagonal gibbsite-like lattice of aluminum hydroxide, whereas the inner walls are lined with an ordered array of pendant silanol groups (Mukherjee et al., 2005). These materials are synthesized under much milder conditions in comparison to CNTs, specifically by hydrothermal methods at ~100 °C and mildly acidic pH. An aluminogermanate analog is also known, with the silicon atoms replaced by germanium. The latter material has recently also been obtained in double-walled form (Thill, 2012a, 2012b). The last decade has seen significant progress in the understanding and manipulation of the growth mechanisms of these materials by controlling the shape and identity of the molecular and nanoscale precursors responsible for nanotube formation (Yucelen et al., 2011). Metal oxide nanotube diameters can now be controlled with Ångstrom-level precision (Yucelen et al., 2012). Their lengths are tunable in a wide range of approximately 20–800 nm. Furthermore, the hydroxylated inner and outer surfaces are amenable to modification by a number of grafting reactions (Kang et al., 2011a, 2011b) to introduce different types of functional groups. Organic-functionalized aluminosilicate nanotubes have also been produced by direct synthesis, thereby yielding nanotubes with organosilane groups replacing the silanol groups in the inner wall (Bottero et al., 2011). Fig. 2c summarizes different approaches available to produce single-walled metal oxide nanotubes with controlled nanotube curvature and composition.

2.2. Layered oxide (2D) materials

Layered materials have created recent interest as molecular sieves and heterogeneous catalysts, because they can be exfoliated/delaminated into single-layered (or few-layered) nanostructures, and can provide many functional sites with a large surface area (Liu, 2007; Centi and Perathoner, 2008; Dasgupta and Torok, 2008). Clays are representative *nonporous* layered materials. A single sheet of a typical clay material has a thickness of ~1 nm, and the structure typically includes two 'tetrahedral' sheets (*i.e.*, with elements such as Si and Al in tetrahedral coordination with oxygen) sandwiching an inner 'octahedral'

sheet. The valency difference between atoms such as Al and Mg in the octahedral layer imparts a net negative charge to the layer and also creates active sites for catalytic applications (Paul and Robeson, 2008). Clays have been used as heterogeneous catalysts by intercalating them with a metal complex (Pinnavaia, 1983). The spacing between individual clay sheets can be expanded using appropriate swelling agents such as surfactants, and can then be 'pillared' by additional silica incorporation to create microporous/mesoporous materials (Kloprogge, 1998). Clays can also be exfoliated after swelling, by application of mechanical force or dispersion in a suitable solvent. Exfoliated clays have been incorporated in polymer matrices to improve the mechanical and chemical properties of engineering plastics (Usuki et al., 1993; Messersmith and Giannelis, 1994) or to improve barrier properties (Choudalakis and Gotsis, 2009). For example, the problem of methanol crossover in sulfonated fluoropolymer (*e.g.*, Nafion®) membranes (Rhee et al., 2005; Thomassin et al., 2006, Lin et al., 2007) can be mitigated by the inclusion of exfoliated clay materials to create a barrier for methanol permeation, leading to more efficient membranes for direct methanol fuel cells (DMFCs).

2.2.1. MCM-22, ITQ, and Nu-6

MCM-22 is a porous layered material with a 10-membered ring (MR) pore structures along two lateral directions and 6MR pores along the vertical direction, as illustrated in Fig. 3a (Leonowicz et al., 1994). Corma (1998) reported swelling methods for MCM-22 using surfactant intercalation, and exfoliated the resulting material to single layers, thereby obtaining a new layered material named ITQ-2. The material MCM-36 has been introduced by pillaring MCM-22 after the swelling process (He et al., 1998). Exfoliated MCM-22 (ITQ-2) is quite attractive for high performance heterogeneous catalysis, due to its large surface density of active sites. Also, it is useful as a molecular sieve for H_2, due to its 6-membered rings perpendicular to the layers. The direct deposition of MCM-22 flakes has been used to form prototype H_2 separation membranes (Choi and Tsapatsis, 2010). Different kinds of exfoliated materials such as ITQ-6, ITQ-18, and Nu-6(2) have been developed starting from layered versions of zeolites Ferrierite and Nu-6 (Corma et al., 2000, 2001) respectively. For example, the layered zeolite Nu-6, which contains 8MRs with 0.33 nm pore openings, can be directly exfoliated during ion exchange of its bipyridine structure-directing agent (SDA) with ions such as Na^+ and CTA^+ at mild pH (~9) and room temperature (Gorgojo et al., 2011).

2.2.2. AMH-3

AMH-3 is the first 3D-porous layered silicate/layered zeolite, having 8 MR pores in all three principal crystallographic directions (Jeong et al., 2003). Fig. 3b shows the pore structure of AMH-3 materials, with the charge-balancing cations removed for clarity. Single layers of AMH-3 of thickness ~1 nm are spaced by charge-balancing Na^+ and Sr^{2+} cations (not shown). AMH-3 is an attractive candidate for membranes containing 'selective flakes', because its 3-dimensional 8MR pore openings are of the appropriate range for various gas separations. The nominally 0.34-nm pore openings of AMH-3 can be applied to various combinations of separations involving gases such as H_2 (kinetic diameter 0.29 nm), CO_2 (0.33 nm), O_2 (0.35 nm), N_2 (0.36 nm), and CH_4 (0.38 nm). A number of challenges have been addressed to apply AMH-3 in

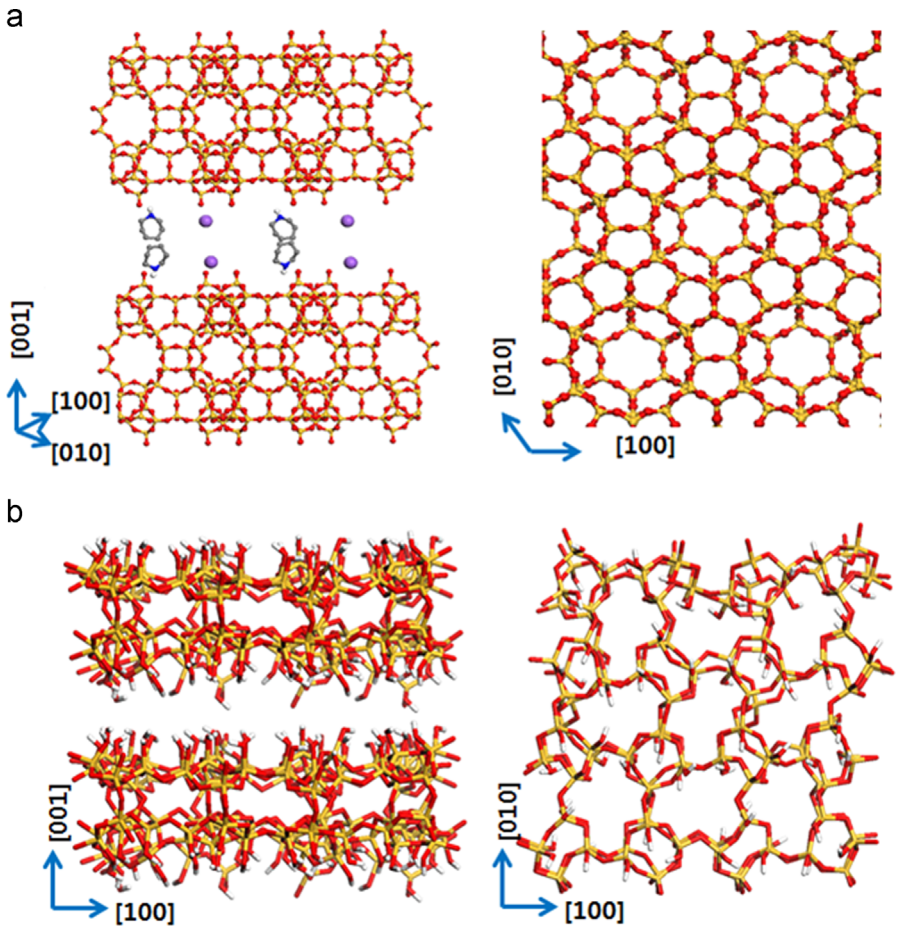

Fig. 3. Structures of nanoporous layered silicates: (a) MCM-22 and (b) AMH-3.

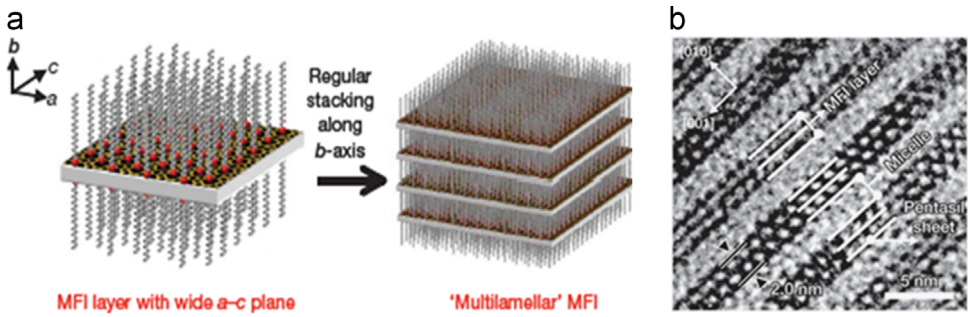

Fig. 4. (a) Schematics of layered MFI assembly and (b) layered MFI structure visualized by high resolution-transmission electron microscopy (adapted from Choi et al., 2009b).

actual gas separation membranes. Unlike most other layered silicate materials, the swelling of AMH-3 is impeded by the strongly bound Na^+ and Sr^{2+} cations between layers. A 'sequential intercalation' method (Choi, 2008a, 2008b, 2008c) has been developed to overcome this difficulty. It involves the controlled ion exchange of the interlayer cations with protons from a buffered solution, followed by the introduction of a primary (rather than quaternary) amine surfactant such as dodecylamine between the layers. However, this process cannot avoid structural changes occurring in swollen AMH-3, involving intra-layer condensation of terminal Si-OH groups (Choi, 2008a, 2008b, 2008c). More recently, it has been shown that the use of a primary diamine surfactant (such as dodecyldiamine) allows better preservation of the AMH-3 layer structure (Kim et al., 2011). The functionalization of swollen AMH-3 surfaces with silane reagents containing hydrocarbon chains also improved its hydrophobicity and may allow better compatibility with hydrophobic polymer matrices.

2.2.3. Layered MFI

Layered MFI is the most recently proposed nanoporous layered material. This material was obtained by synthesizing a new SDA that is terminated with a long-chain C_{22} alkyl group (Choi et al., 2009b). The amine groups in the SDA allow the formation of an MFI structure in the lateral directions (crystallographic *ac*-plane) in a manner similar to the conventional tetrapropylammonium SDA, but the long-chain alkyl group prevents crystal growth in the perpendicular (crystallographic *b*-axis) direction (Fig. 4a). Hence, a layered material containing 2 nm thin MFI sheets could be synthesized in a one-step hydrothermal reaction. Layered MFI has the same pore size and local structure as conventional MFI, *i.e.* 10MR pores with a nominal pore size of 0.55 nm (Diaz, 2004). This relatively larger pore size (in comparison to MCM-22 and AMH-3) can be applied to the separation of bulkier molecules such as hydrocarbons or other organics. Moreover, as shown in Fig. 4b, layered MFI has an already swollen structure since the MFI layers are spaced by the long-chain alkyl groups of the SDA. This may be an advantage for utilization of this material in membrane fabrication applications, since it avoids the need for swelling processes involving ion exchange, surfactant intercalation, and other steps. By controlling the Na^+ content in the reaction gel, two different types of layered MFI – multilamellar and unilamellar – have been synthesized. The pillaring process for layered MFI has expanded its potential applications in heterogeneous catalysis (Na et al., 2010). Layered MFI has also been combined with conventional MFI in the form of a hybrid BMLM (bulk MFI-layered MFI) material. This material is synthesized by epitaxial growth of layered MFI on conventional MFI crystal surfaces (Kim et al., 2012a, 2012b). The growth of layered MFI on bulk MFI has been found to occur in all three principal crystallographic directions, and involves both homoepitaxial and heteroepitaxial growth.

2.2.4. Layered titanosilicates and aluminophosphates

Apart from layered nanoporous silicates, other layered oxide materials such as titanosilicates and aluminophosphates (AlPOs) have also been synthesized. The layered titanosilicate JDF-L1 (Roberts et al., 1996) contains 6MRs formed by two TiO_5 square pyramids and four SiO_4 tetrahedra, and whose pore openings of ~0.3 nm may be suited for selective hydrogen permeation. Using a sequential intercalation process similar to that developed for AMH-3, this material has been successfully exfoliated by proton exchange from a buffered histidine solution followed by intercalation of nonylamine and final extraction with an HCl/ethanol/water solution (Rubio et al., 2010). Layered AlPO materials also have potential applications in catalysis (Thomas et al., 2001) and in fabrication of nanocomposite materials and membranes (Jeong et al., 2004). By varying the SDA, porous AlPO materials can be synthesized in different forms such as 1D chains, 2D layers, and 3D open frameworks (Williams et al., 1997; Yu et al., 1998a, 1998b; Li et al., 1999). The dimensionality, pore structure, and composition of the AlPO are influenced by the size and shape of the organic (usually amine) SDA (Li et al., 1999). The 2D (layered) AlPOs have negatively charged layers with Al:P ratios less than unity, in comparison with 3D AlPOs with an Al:P ratio of unity. The anionic AlPO layers contain AlO_4 tetrahedra and $O{=}PO_3$ (PO_4) units with corner-shared oxygen atoms, to form AlPO materials with varying Al:P ratios (Williams et al., 1996; Yu et al., 1998a, 1998b; Yan et al., 2000). The SDA molecules (such as trimethyl-, triethyl-, or isopropanolamine) interact with the AlPO layers *via* non-covalent bonds, and hence the 2D layers can be delaminated to single layers for the fabrication of nanocomposite membranes. However, unlike the slab-like layered silicate materials described above, the AlPO layers have more fragile net-like morphologies of thickness ~0.5 nm, leading to lower chemical stability upon swelling and exfoliation.

2.3. Graphene-based materials

Graphene is a single-atom-thick 2D carbon material with a graphitic hexagonal layer structure. It has a network of sp^2 hybridized carbon atoms that leads to a zero bandgap and enables the fast transport of electrons. Since graphene was first isolated from graphite sheets by mechanical exfoliation methods (Novoselov et al., 2004), scientific interest in its electrical, optical and mechanical properties has grown extremely fast (Bunch et al., 2007; Staley et al., 2007; Liu et al., 2009). High Resolution-Transmission Electron Microscopy (HRTEM) visualizes the single and bilayer graphene sheet as shown in Fig. 5a (Urban, 2011). Utilization of graphene as an additive material requires larger-scale production of graphene sheets. Single-sheet graphene was obtained from graphite oxide by a reduction process using hydrazine (Tung et al., 2009). Apart from the developments on utilizing graphene directly grown on substrates for electronic/optical

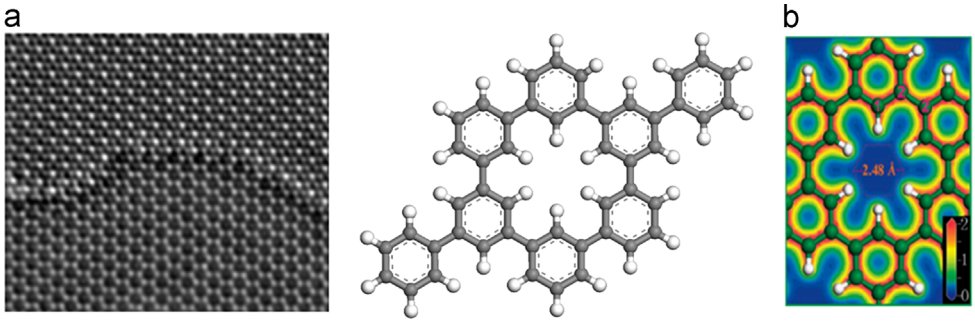

Fig. 5. (a) HRTEM image of single and bilayer of graphene (adapted from Urban, 2011), and (b) schematics of porous graphene structure.

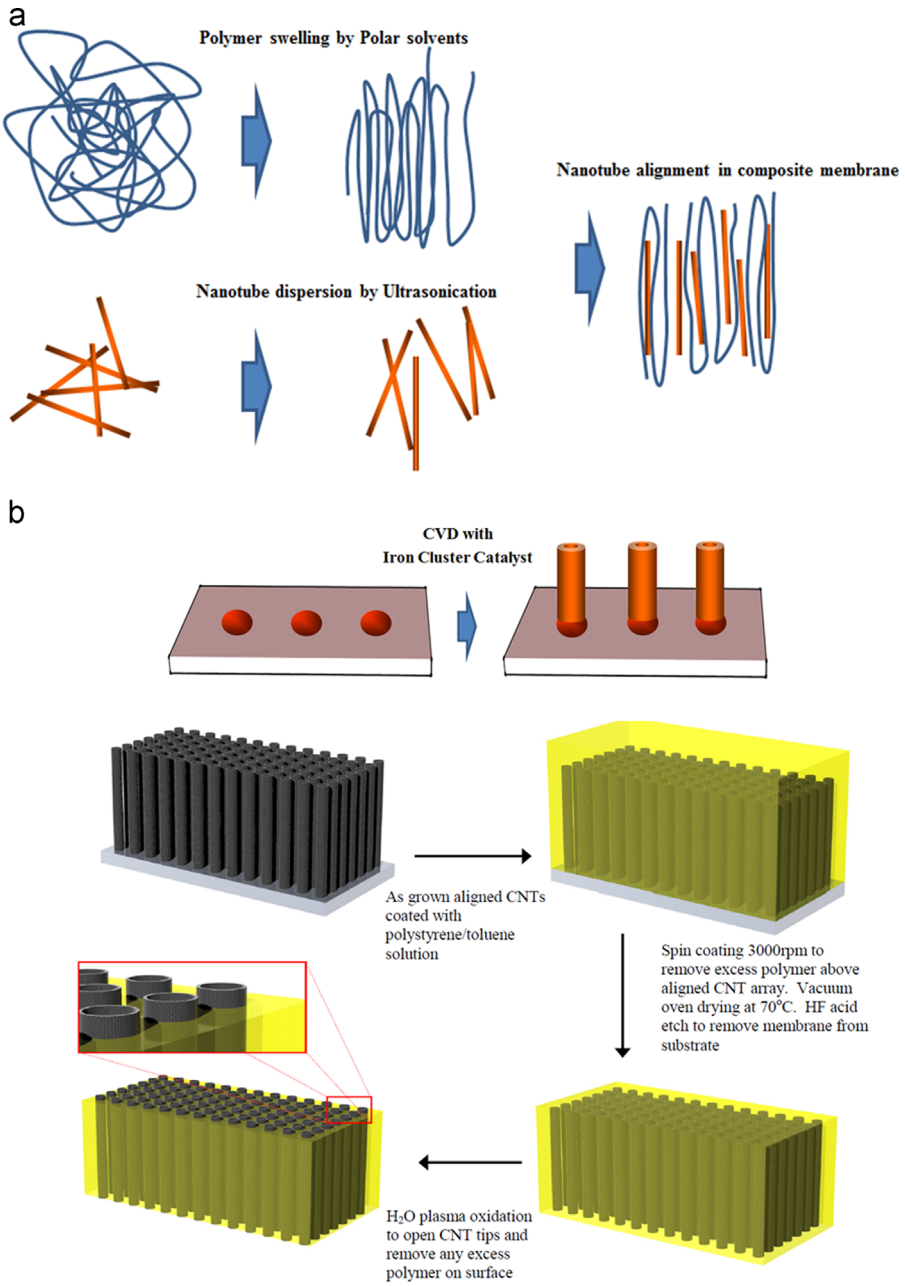

Fig. 6. Fabrication processes for nanotube/polymer composite membranes using (a) solution casting method, and (b) CVD method followed by polymer coating and etching process (adapted from Majumder et al., 2011).

applications (Allen et al., 2010; Shao et al., 2010), another important potential application of bulk-processed graphene is in the form of separation membranes (Blankenburg et al., 2010). The one-atom-thin layer structure and strong mechanical properties are attractive for application in molecular separation. However, as shown in Fig. 5a, graphene sheets do not have pores for molecular sieving. The

introduction of sub-nanometer pores is required to obtain sufficient molecular permeance and to control the permselectivity. As a proof-of-concept, electron beam lithography has been used to create holes in suspended graphene sheets (Fischbein and Drndic. 2008). However, this 'top-down' fabrication method is hard to control and often not precise. 'Bottom-up' assembly processes are also being considered for the formation of porous 2D sheets of graphene (Bieri et al., 2009). For example, as shown in the schematic of porous graphene (Fig. 5b), phenylene molecules can be used as building units for porous grapheme (Li et al., 2010). Computational studies have been performed to calculate the separation properties in porous graphenes, indicating interesting molecular sieving possibilities (Jiang et al., 2009; Blankenburg et al., 2010, Li et al., 2010; Schrier, 2010). The use of few-layer graphene (rather than monolayer graphene) may also lead to other interesting possibilities for molecular separation. However, this form of graphene is less commonly considered for composite film formation in the current literature (Prolongo et al., 2013).

3. Processing of membranes containing 1D and 2D materials

After the preparation of well-defined 1D (nanotubular) and 2D (layered) porous materials, there are several steps in the formation of membranes utilizing these materials. In this section, we consider processing methodologies for fabricating both nanocomposite and single-phase membranes with low-dimensional porous materials.

3.1. Nanocomposite membranes

3.1.1. Composite membranes with nanotubes

In nanotube/polymer composite membranes, the highest performance in terms of molecular selectivity and permeability can be attained by the simultaneous dispersion and alignment of nanotubes in polymer matrix, as illustrated in Fig. 1a. Several approaches using physical and chemical methods have been reported to align CNT arrays in polymer matrices. One example is the alignment of CNTs during solvent casting (Chen and Tao, 2005). The relaxation and alignment of polymer chains during the swelling and curing stages of solvent casting can be used for the alignment of CNT arrays, as illustrated in Fig. 6a. This process is potentially advantageous for scale-up. However, it currently suffers from several problems, such as the difficulty in controlling the uniformity of the final membrane. A CVD process for aligned growth of a nanotube 'forest' using iron clusters as the catalysts, followed by infiltration of the intertube spaces with a polymer (Fig. 6b), has also been suggested. Composite membranes with well-aligned CNTs have been fabricated with the above process (Cheung et al., 2002). This method can provide high quality membranes; however, the scale-up of the CVD process is challenging. Other methods for the alignment of nanotubes employ shear flows or electric fields (Pujari, 2009; Mauter et al., 2010). The deposition of CNTs on substrates (that have different surface properties from the nanotubes) has been shown to result in vertical alignment (De Heer et al., 1995; Kim et al., 2007).

Apart from CNTs, there has been a recent demonstration of the fabrication of composite membranes using single-walled aluminosilicate nanotubes (Fig. 2b) dispersed in a hydrophilic polymer (polyvinylalcohol) (Kang et al., 2012). The hydrophilic nature of the nanotube material allows excellent dispersion in the polymer solution. Since no driving force was present for nanotube alignment, the resulting membranes showed a random orientation of the nanotubes in the polymer matrix. Similarly, hydroxyl-functionalized multiwalled CNTs (MWNTs) have also been well dispersed *via* formation of covalent linkages to a copolyimide (6FDA-4MPD/6FDA-DABA 4:1) matrix under ultrasonication, thereby allowing the formation of a composite membrane (Sieffert and Staudt, 2011). There is no evidence for a preferential orientation/alignment of the MWCNTs in the membrane.

3.1.2. Composite membranes with porous layered oxides

For both nanocomposite and all-inorganic membrane fabrication utilizing layered oxides, controlling the exfoliation of the layers is important. As-synthesized or surfactant-swollen layered materials usually comprise stacks of 100-10,000 layers. Depending on the degree of exfoliation, the final processed layered materials (flakes) can be defined (Paul and Robeson, 2008) as either (1) 'immiscible' (essentially unaltered from their as-synthesized or swollen state), (2) 'intercalated' (having polymer chains threaded between the layers which still maintain some registry with each other), or (3) 'exfoliated' (with individual layers or few-layer stacks separated from each other and dispersed). There are many studies on polymer/clay composite materials for applications to mechanical reinforcement and enhancement of barrier properties (Ray and Okamoto, 2003; Schaefer and Justice, 2007; Vaia and Maguire, 2007; Pavlidou and Papaspyrides, 2008). These studies contain considerable insight into intercalation and exfoliation processes for clay materials, which has served as a useful starting point for work on exfoliation of porous layered materials.

Melt-blending, a technique used in the majority of studies on exfoliation of clay materials in polymers, is also an attractive method for exfoliative dispersion of porous layered materials in polymers. It involves the use of different types of screw extruders to blend molten polymers and layered materials at temperatures near 400 °C. The results depend strongly on the melt-blending conditions, the affinity between the polymer and clay, and the extruder type. Specifically, layered MFI powders (Fig. 7a) have been incorporated in polystyrene and melt-blended using a twin screw extruder. As a result (Fig. 7b), it was found that the single layers of layered MFI have been completely exfoliated (Varoon et al., 2011). However, the technique is not directly applicable to the fabrication of nanocomposite membranes for separations, since the polymers required for permselective membranes (*e.g.*, polyimides, cellulose acetate, polyvinylalcohol) are usually solution-processed and not melt-processable. Previous attempts to exfoliate porous layered materials in solution (*i.e.*, solution-blending) have encountered problems such as strong aggregation of the layered materials (Krikorian and Pochan, 2003; Ray and Bousmina, 2005; Pavlidou and Papaspyrides, 2008). Similar to the illustration in Fig. 6a, the conventional solution blending process includes the intercalation of polymer chains between layers, followed by membrane casting and solvent evaporation. An active exfoliation process can be added to the conventional solution blending process. For example, it has been recently shown that high-shear mixing can be used to exfoliate swollen AMH-3 (Fig. 7d and e) in solution during blending with cellulose acetate. Fig. 7f shows a TEM cross-section image of the membrane forming after the casting step. The stacked layers of swollen AMH-3 have been converted to few-layer flakes dispersed in the cellulose acetate matrix (Kim et al., 2013).

Other potential methods for membrane fabrication with exfoliated porous layered materials include *in situ* polymerization and sol-gel processing. *In situ* polymerization was used to fabricate clay/Nylon-6 composite materials (Usuki et al., 1993). The concept was to polymerize the monomer in the gallery spaces of layered materials and thereby expand their *d*-spacing, eventually resulting in delamination. An advantage of this method is the capability to control the polymerization rate and exfoliation conditions. Using ring-opening polymerization of cyclic oligomers, the degree of exfoliation of clay materials showed significant improvements (Lee

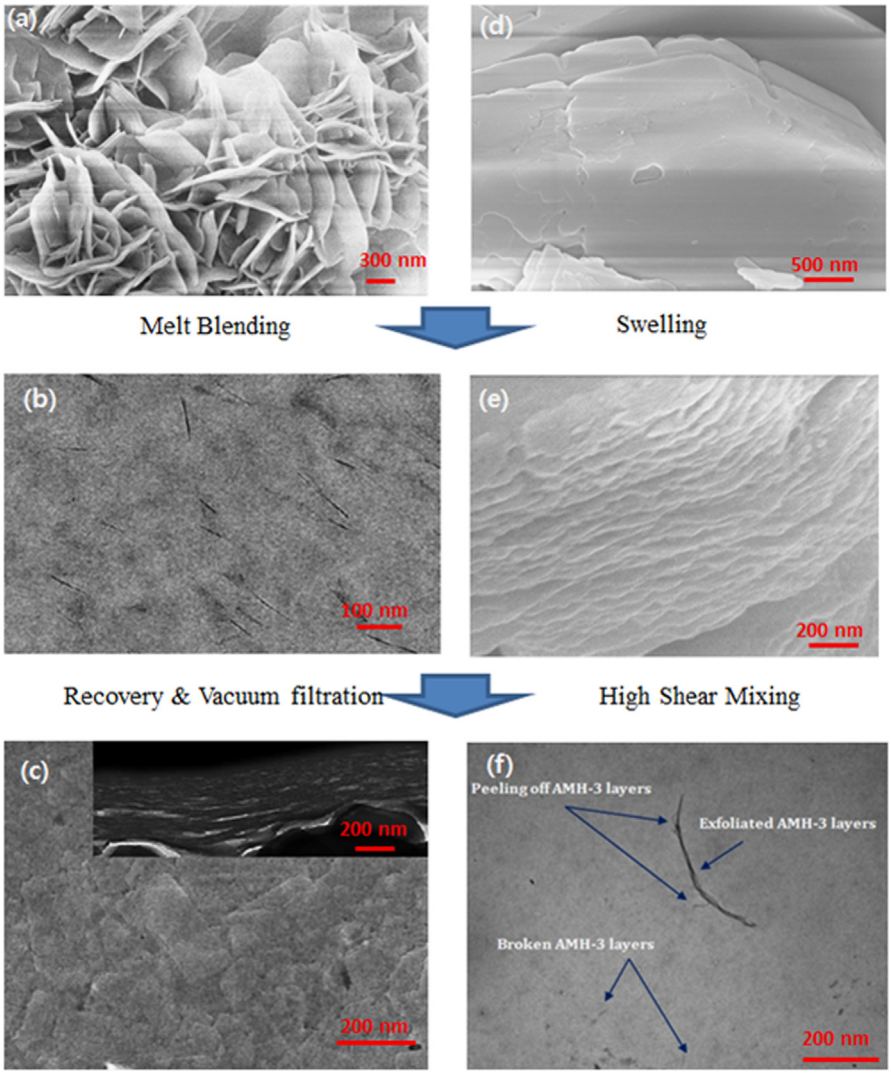

Fig. 7. Exfoliation and membrane fabrication processes using (a–c) layered MFI (adapted from Varoon et al., 2011), and (d–f) SAMH-3 (adapted from Kim et al., 2013). The initial as-made layered MFI and AMH-3 (a and d) have been delaminated to single-layer and few-layer flakes respectively (b and e); and (c and f) subsequently fabricated into all-inorganic layered MFI and cellulose acetate/AMH-3 composite membranes respectively.

et al., 2005). While the *in situ* polymerization method involves only the polymerization of monomers, the sol–gel process includes both the polymerization reaction and crystal growth of the inorganic particles at the same time (Pavlidou and Papaspyrides, 2008). Neither of these techniques has yet been applied to porous layered materials.

3.2. All-inorganic membranes

Apart from their processing into nanocomposite membranes, nanoporous layered materials after exfoliation can be used to form inorganic membranes on porous substrates. Methods for the fabrication of inorganic membranes using exfoliated layered flakes are layer-by-layer (LBL) dip coating, spray coating, spin coating, and vacuum filtration. There are several examples of the formation of inorganic membranes from porous layered materials. MCM-22 flakes were exfoliated and then coated on α-alumina substrates using LBL dip coatings followed by TEOS vapor post-treatment (Choi and Tsapatsis, 2010). The latter step was required in order to fill microscopic gaps (defects) between coated layers. Because the MCM-22 flakes have a high aspect ratio and significant interlayer interactions, the 6MR pores of the successively coated MCM-22 layers were found to be approximately aligned perpendicular to the substrate with *c*-axis out-of-plane orientation. After post-treatment with TEOS vapor, the membrane displayed H_2/N_2 separation with high selectivity of 120. In another example, the exfoliated flakes of layered MFI embedded in polystyrene after melt blending (Fig. 7b) were recovered by dissolution of the polymer in an organic solvent, and were then deposited as coatings on porous supports using vacuum filtration (Fig. 7c) (Varoon et al., 2011). The initial coatings were not permselective due to the presence of gaps between layers. To improve the separation properties, the coated membranes were post-treated with a silica-containing solution by hydrothermal growth, to close the gaps by growth of crystalline MFI. The resulting membranes showed high selectivity for *p*-xylene over *o*-xylene (Section 4). Multilayer graphene membranes have been fabricated by spin coating or spray coating of graphene oxide suspensions on copper substrates, followed by etching using nitric acid (Nair et al., 2012). Also, a prototype single-sheet porous graphene membrane has been fabricated by the combination of photolithography and mechanical exfoliation of graphene with a cellophane tape (Koenig et al., 2012). The subsequent UV-oxidative etching step introduced sub-nanometer pores in the graphene sheet.

3.3. Microstructural analysis of nanocomposite membranes

An important aspect of nanocomposite membrane studies is the determination of the membrane microstructure. This is particularly challenging in the case of membranes containing 1D and 2D porous materials. Microstructural characterization should reveal the degree of exfoliation of 2D flakes, the dispersion quality of flakes or 1D nanotubular materials in the polymer matrix, their degree of orientation, and the interface quality/adhesion between the polymer and low-dimensional inorganic fillers. These characteristics are intimately connected to the ultimate separation performance of the nanocomposite membrane (Schaefer and Justice, 2007; Vaia and Maguire, 2007). Here we review some of the representative microstructural analyses on composite membranes incorporating nanoporous 1D and 2D materials.

Wide Angle X-ray Scattering (WAXS) can be used to determine the *d*-spacings of layered materials dispersed in polymers, and it can be a qualitative indication of the degree of exfoliation (Paul and Robeson, 2008). The crystallinity of the polymeric phase in the composite membrane can be determined by deconvolution of the WAXS patterns to determine the fractions of crystalline and amorphous polymer. Crystallinity changes in the polymer matrix correlate with changes in the polymer chain packing, and can lead to interesting modifications of the separation properties in addition to the effect of the inorganic material (Kang, 2012). However, the characteristic peaks seen in WAXS may depend strongly on measurement conditions such as scanning time and detector type. Misleading quantitative results can be obtained from WAXS patterns, and they should be considered as qualitative information (Paul and Robeson, 2008).

On the other hand, small angle X-ray and neutron scattering (SAXS/SANS) measurements can give detailed microstructural information, and have been widely used for analyzing the microstructure and morphology of polymeric and composite materials. To highlight a specific case of polymeric membranes, SAXS analysis gave detailed information on the structure (specifically, the size and orientation of water nanochannels) of ionic polymers such as Nafion® and sulfonated polyimides (Gebel and Diat, 2005; Schmidt-Rohr and Chen, 2008). The structure and morphology of cellulose acetate membranes has also been studied by SANS, and the results have compared well to transmission electron microscopy (TEM) analysis (Kulkarni et al., 1994). Beyond the characterization of polymer microstructure, SAXS/SANS analysis can give morphological information on polymer/inorganic composite membranes. The slope of SAXS/SANS patterns in the low momentum transfer (Q) regions is a quantitative indication of the dispersion and morphology of embedded 1D and 2D materials. The Q-dependence of single exfoliated 2D layers is expected to have a power law exponent of -2, and the exponent is expected to become steeper as the degree of exfoliation and dispersion decreases (Kratky and Porod, 1949). For example, a MMT/PA66 composite (whose TEM image is shown in the inset of Fig. 8a) has a steeper exponent of -3 at low Q (Fig. 8a), due to the presence of globular clusters of exfoliated clay flakes. Similarly, an AlPO/polyimide composite membrane (Jeong, 2004) showed a slope of -3.5, corresponding to multi-layer particles (10–100 nm in size).

Detailed scattering model fits quantitative morphological information. A variety of X-ray/neutron scattering model equations have been developed based on the geometry of the inorganic fillers, *e.g.*, spheres, disks/layers, rods (Kratky and Porod, 1949; Wang et al., 2007). SAXS data from composite membranes containing single-walled aluminosilicate nanotubes in PVA has been fitted in detail to a model of scattering from rod-like dispersed objects to obtain morphological characteristics such as the average intertubular distance and nanotubular particle dimensions (Kang et al., 2012). This analysis, together with WAS patterns, clearly revealed a near-perfect dispersion of individual nanotubes in the membrane even at high loadings (up to 40 vol%). The WAXS patterns also revealed a decrease in the crystalline:amorphous ratio of the cellulose acetate phase with increasing nanotube loading, thereby indicating significant changes in the polymer packing induced by the nanotube fillers. On the other hand, the stacked-tactoid model is applicable to the case of composite membranes containing 2D flakes (Ho et al., 2001; Hanley et al., 2003). The scattering model consists of the form factor and structure factor of the flake. The form factor includes information on flake dimensions and orientation, and the structure factor describes the internal morphology of the flakes, such as the average number of layers in the flakes and the interlayer spacing. The structure factor can also be convoluted with probability distributions such as Gaussian functions to capture the statistical variations in the number of layers and interlayer spacing in the sample. Fig. 8b (Kim et al., 2013) shows SAXS model fitting results from AMH-3/cellulose acetate composite membranes at different AMH-3 loadings. The analysis demonstrated a high degree of exfoliation of the AMH-3 flakes in relation to the initial swollen

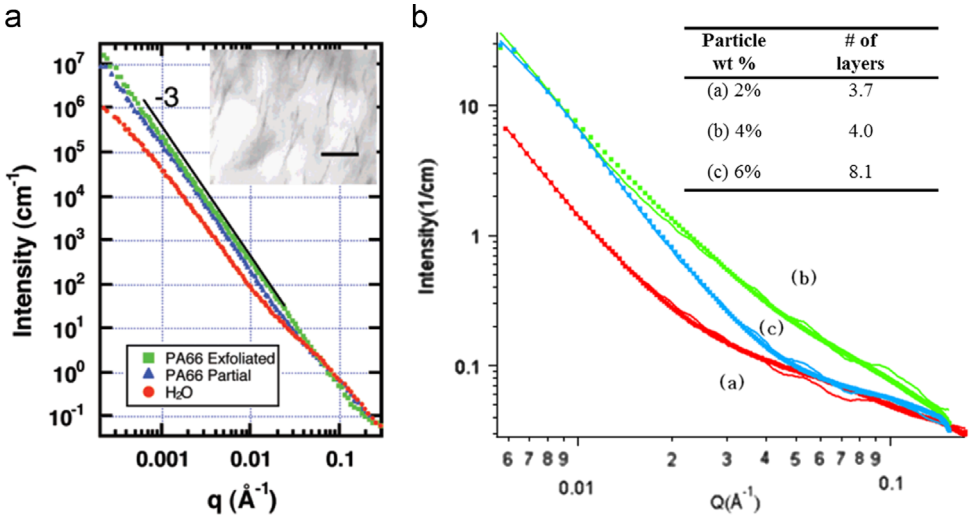

Fig. 8. SANS analysis of (a) PA66/MMT composite material (adapted from Schaefer and Justice, 2007), and (b) SAXS model fitting to analyze the degree of exfoliation of swollen AMH-3 in cellulose acetate (adapted from Kim et al., 2013). The inset table shows the average number of layers in the AMH-3 flakes obtained from the SAXS analysis at different loadings of AMH-3 in the membrane.

material (Fig. 7e). The dispersed AMH-3 flakes contain (on the average) 4–8 layers. Further details of the statistical variation of the number of layers and the interlayer spacings were also obtained. Similar analyses have been demonstrated for membranes containing clay platelets (Yoonessi et al., 2005).

Other characterization techniques can also yield considerable insight on the composite microstructure. ^{1}H-NMR can be used to trace the degree of exfoliation and alignment of layered materials in composite membranes. For example, Xu et al. (2009) measured ^{1}H spin-lattice relaxation times in clay/polypropylene composites and thereby tracked the evolution of clay morphology (specifically, the exfoliation and alignment of montmorillonite) induced by equibiaxial stretching of the composite. Polarized Raman spectroscopy has also been employed to deduce a preferential horizontal (in-plane) orientation of JDF-L1 titanosilicate layers in a copolyimide membrane matrix (Galve et al., 2011). Raman spectra were measured with light sources polarized either parallel or perpendicular to the membrane plane. The comparison of vibrational Raman peak intensities of the polymer chains as well as the JDF-L1 layers under the two measurement conditions indicated a preferred horizontal orientation for the JDF-L1 flakes. HRTEM is also a useful method to examine the dispersion of layered materials in a polymer matrix. Its main drawback is that it can only image very small portions of the sample at a time and hence does not produce statistically valid results. Hence, it should be combined with more statistically sound techniques such as SAXS/SANS, NMR, and Raman spectroscopy to develop a reliable picture of the nanocomposite membrane microstructure.

4. Separation applications

As mentioned earlier, the pore structures of nanoporous 1D and 2D materials are attractive for obtaining molecular separation properties. A number of separations applications of membranes containing these materials have been investigated. This section highlights advances in gas separation, water purification, organics purification, and proton conduction by membranes containing nanoporous 1D and 2D materials. Throughout the following discussion, different mechanisms of molecular separation operating in these materials are illustrated. Broadly speaking, the 1D nanotubular materials provide molecular transport paths of lengths greater than ~10 nm, and hence display adsorption and diffusion-based selectivity behavior similar to that observed in nanoporous materials like zeolites and metal-organic frameworks (MOFs). On the other hand, the ~1 nm thin layers found in the 2D nanoporous materials provide much shorter, discontinuous, molecular transport paths that likely cannot be described in the same manner as transport in zeolites and MOFs. This issue is highlighted in Section 4.2 with several examples.

4.1. 1D nanotubular membranes

Several molecular simulation studies have indicated that nanotubular materials can be attractive candidates for gas separations (Skoulidas et al., 2002; Sokhan et al., 2004; Matranga et al., 2006) as well as liquid separations (Sokhan et al., 2002; Konduri et al., 2008). A macroscopic model of permeation has also been recently developed for membranes containing 1D nanotubular fillers, and the effects of parameters such as the nanotube orientation distribution, aspect ratio, volume fraction, and membrane defects, have been assessed in detail *via* this model (Kang, 2011a, 2011b). The above works have indicated that nanotube-containing membranes are capable of significant enhancements in molecular flux and potentially in selectivity over polymeric membranes. Membranes containing carbon SWNTs and MWNTs have been investigated for gas/vapor-phase and liquid-phase separations (Cong et al., 2007). The incorporation of SWNTs and MWNTs in brominated poly(2,6-biphenyl-1,4-phenylene oxide) polymeric membranes significantly improved the CO_2 gas permeability while maintaining a high CO_2/N_2 selectivity (Fig. 9). Additionally, the incorporation of CNTs in the polymer matrix improved the mechanical properties of the membrane, such as the tensile modulus. The latter results were attributed to the favorable interactions of the outer walls of the CNTs with the biphenyl groups of the polymer. Separation of water from ethanol has also been investigated using CNT/PVA composite membranes (Fig. 10a) (Choi et al., 2007). The water flux increases while the water/ethanol separation factor decreases, as nanotube loading increases. These results can be rationalized by the fact that CNTs are known to allow very high fluxes (by virtue of their atomically smooth walls) of many molecules such as water, other polar molecules, and hydrocarbons (Majumder et al., 2011). This property also renders them unselective for mixtures such as water/ethanol. On the other hand, it has been shown recently that selectivity can be imparted to CNTs by modifying their ends with functional groups. For example, the modification of CNT ends with zwitterions (containing carboxylate and tertiary amine groups), followed by the incorporation of the modified CNTs into a polyimide matrix, resulted in membranes that retain the expected high water flux and also achieve approximately 99% rejection of salt ions (Chan et al., 2013). The zwitterionic modifying groups allow water molecules to pass through but block the permeation of ions by charge repulsion and steric hindrance.

The uniformity of nanotube dispersion in the polymer is also important for performance enhancement. For example, carbon nanotube/polymer composite membranes containing aggregated

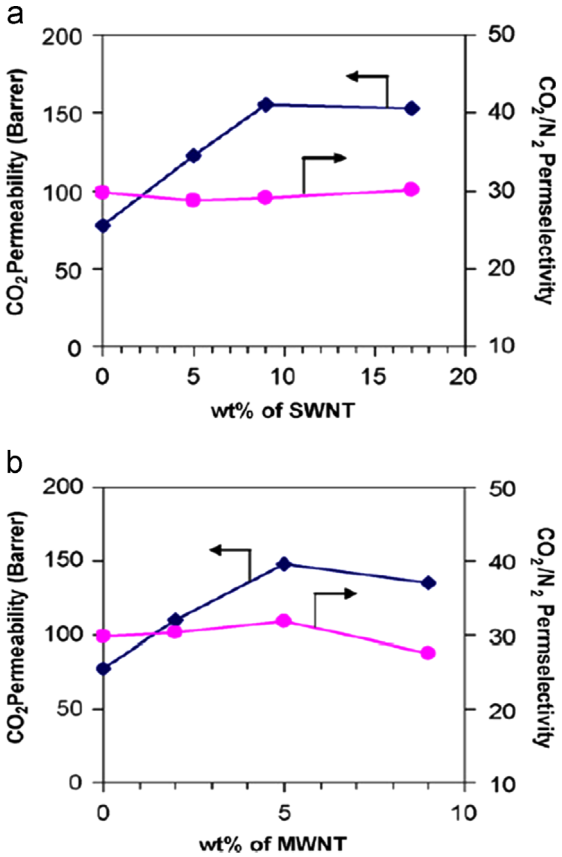

Fig. 9. CO_2/N_2 separation performance of composite membranes incorporating (a) SWNT, and (b) MWNT in a brominated poly(biphenylphenylene oxide) polymer matrix. (Adapted from Cong et al., 2007).

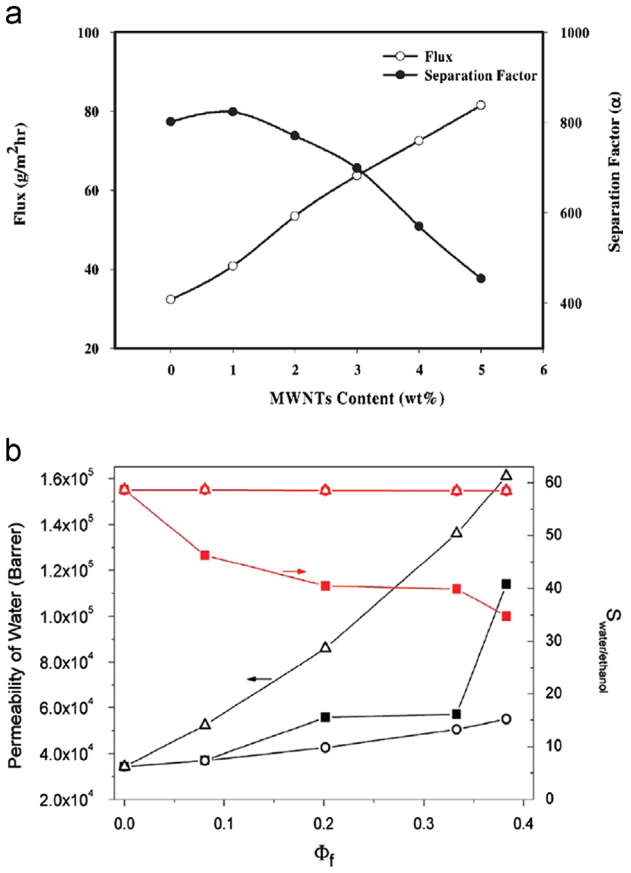

Fig. 10. Water/ethanol pervaporation performance of PVA membranes incorporating (a) CNTs (adapted from Choi et al., 2007) (b) and aluminosilicate nanotubes (adapted from Kang et al., 2012).

nanotubes have low molecular selectivity. To address the problem of increasing the nanotube loading in nanocomposites while maintaining good dispersion, a range of techniques for outer surface modification of carbon nanotubes have been developed (Dyke and Tour, 2004; Zhao and Stoddart, 2009; Clavé et al., 2013) that can enhance the nanotube compatibility with the polymeric matrix. Nevertheless, the highest volume fraction reported to date of CNTs dispersed in a polymeric material without significant nanotube aggregation is only about 20% (Jain, 2010; Chan, 2013). This limitation hinders the performance enhancement that CNTs can potentially create in a composite material or membrane. However, individual dispersion of nanotubes in polar liquids can be achieved in the case of single-walled metal oxide nanotubes that have polar surfaces. As mentioned earlier, single-walled aluminosilicate nanotubes (Fig. 2b) are synthesized hydrothermally in water, and have a high degree of dispersion in aqueous media. These SWNTs are hypothesized to be amenable to the fabrication and application of high-loading nanotube composites with near-ideal dispersion of nanotubes. Previous studies have suggested that aluminosilicate NTs possess extraordinarily high interior hydrophilicity due to their high inner surface silanol densities, thereby leading to a high water/alcohol selectivity (Zang et al., 2009, 2010). Single-walled aluminosilicate NT/polyvinylalcohol (PVA) composite membranes have been fabricated and applied to water/ethanol separation by pervaporation (Kang et al., 2012). As described earlier in this work, SAXS and WAXS analysis showed excellent dispersion of the NTs at high loadings (up to 40 vol%). An increased water flux was obtained (Fig. 10b) in comparison to pure PVA, whereas the water/ethanol separation factor (35–45) showed a decrease from PVA and was similar to that of the CNT/PVA membrane. These results are also likely to be influenced by the change in the PVA packing characteristics upon increasing loading of the NTs, which was characterized by XRD and NMR techniques described earlier in this review.

4.2. 2D layered oxide membranes

The first gas separation data from polymer/selective flake composite membranes was reported for the case of porous layered AlPO/polyimide composite membranes (Jeong et al., 2004). The composite membrane showed improvements in O_2/N_2 selectivity, attributed to molecular sieving through the porous layered AlPO. However, SANS analysis showed that the AlPO material was not exfoliated in the polymer. Similarly, swollen AMH-3 was incorporated in polybenzimidazole (PBI), and showed moderate improvements on overall CO_2/CH_4 selectivity attributed to molecular sieving effect of the AMH-3 pores (Choi et al., 2008a, 2008b, 2008c). The layered titanosilicate JDF-L1 has also been incorporated in a copolyimide, and showed significant improvements in H_2/CH_4 separation attributed to molecular sieving through its 0.3 nm pore openings (Galve et al., 2011). In a recent study, (Kim et al., 2013) swollen AMH-3 was significantly exfoliated in cellulose acetate (Section 3.1), and the nanocomposite AMH-3/CA membrane system showed significantly improved CO_2 permeability while maintaining (but not improving) CO_2/CH_4 selectivity even at low loadings (2–6 wt%) of swollen AMH-3 (Fig. 11). This result is attributed to a complex transport mechanism involving transport through the AMH-3 pores as well as the interlayer mesopores in the partially exfoliated stacks of 4–8 AMH-3 layers. The MFI BMLM material (Section 2.2) has also been incorporated into a polyimide matrix and showed superior particle/polymer adhesion properties over the conventional MFI material (Kim et al., 2012a, 2012b). Several characterization techniques revealed the infiltration of the polyimide chains between the layers of the epitaxially grown MFI layers, thereby enhancing the adhesion between the inorganic and polymeric phases. This resulted in superior CO_2/CH_4 separation characteristics over conventional MFI particles dispersed in the same polymer. All-inorganic membranes fabricated with layered zeolites have also been applied to various separations. The *c*-oriented inorganic membranes fabricated from MCM-22 flakes (with 6MR pore openings) have been applied to H_2 separations and showed significant improvements on H_2/N_2 selectivity (Choi and Tsapatsis, 2010). A selective membrane fabricated from exfoliated MWW flakes showed highly improved selectivity in He/N_2 separation attributed to molecular sieving through its 6MR pores (Varoon et al., 2011). Exfoliated layered MFI has been applied to xylene separations, by utilizing its 10MR pore openings (Varoon et al., 2011). A high *p*-/*o*-xylene separation factor of 65 was obtained.

The membrane applications of porous 2D materials have been expanded to ion conducting membranes, such as proton exchange membranes for direct methanol fuel cells (DMFCs). The major components of a DMFC are the anode, the cathode and the proton exchange membrane (PEM). At the anode, methanol is converted to electrons, protons, and CO_2 as a byproduct. The protons are transported through the PEM to the cathode, where they react with oxygen and electrons to produce water. The development of higher-performance PEMs is important to improve the overall DMFC performance (Jagur-Grodzinski, 2007). Specifically, the PEM is required to have high proton conductivity, as well as low methanol permeability (to prevent transport of the fuel through the PEM). The existence of mesoscopic water channels in PEMs made with Nafion® and other sulfonated fluoropolymers (also called ionomers) is important for obtaining good proton conductivity, but they also provide transport paths for methanol crossover as a side effect. Several works have reported the incorporation of clay materials in ionomers (Jung et al., 2003; Rhee et al., 2005; Thomassin et al.,

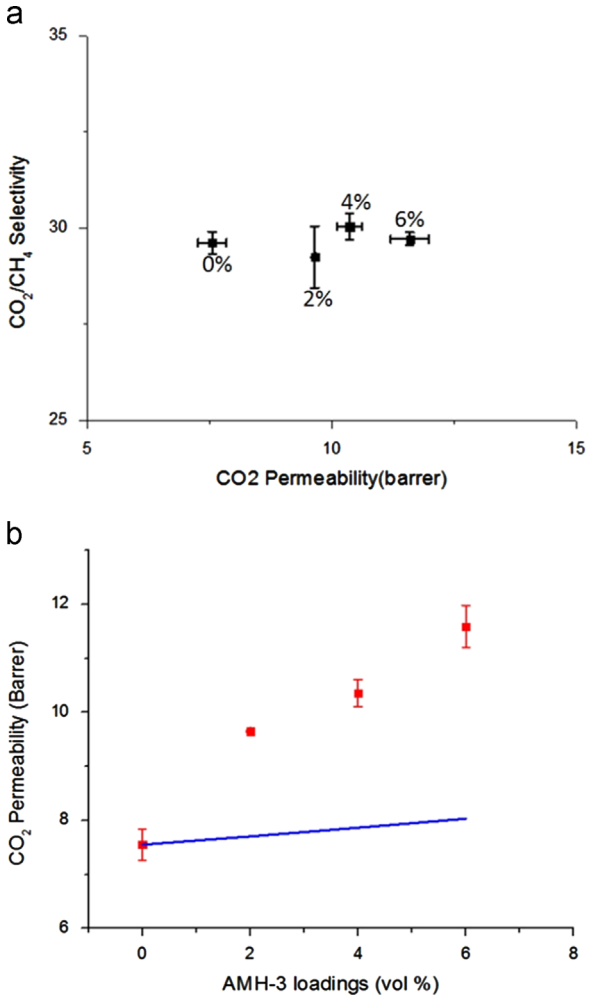

Fig. 11. (a) CO_2/CH_4 selectivity and CO_2 permeability at different AMH-3 loadings, and (b) CO_2 permeability as a function of AMH-3 loading in AMH-3/cellulose acetate (CA) composite membranes at a pressure differential of 65 psi. The solid blue line is the highest possible CO_2 permeability predicted by the Cussler model (adapted from Kim et al., 2013).

2006). However, clays are non-porous layered materials that act as barriers for both protons and methanol, resulting in a trade-off between reduction in methanol crossover and maintenance of proton conductivity. Porous layered oxides may be good alternative materials, as they can permeate the protons through their subnanometer pores. For example, swollen AMH-3 flakes have been incorporated in Nafion® membranes (Hudiono et al., 2009; Kim et al., 2012a, 2012b). A significant (30–50%) decrease in methanol permeability was observed, whereas high proton conductivity was maintained. SAXS measurements also revealed that the incorporation of AMH-3 substantially altered the microstructure of the ionomer (Hudiono et al., 2009). The mechanisms responsible for the improvements in performance (such as molecular sieving through the pores of the layered material, or alteration of the transport properties of the water channels) have not yet been fully clarified.

To predict the effects of incorporation of layered materials on the separation performance of composite membranes, Cussler developed an analytical model for the calculation of permeability and selectivity of gas molecules in composite membranes containing selective flakes (Cussler, 1990). The limits of applicability of this model have been evaluated in detail *via* finite-element simulations of membrane matrices containing flake-like domains in ordered arrangements (Sheffel and Tsapatsis, 2007, 2009). It was found that the Cussler model, including modifications that allow a wider range of flake volume fractions and length:thickness aspect ratios, showed reasonable agreement with finite-element simulations for flakes with aspect ratios greater than about 5. However, an important assumption of both the analytical model as well as the finite-element simulations is that a bulk molecular diffusivity or permeability can be defined for the flake. While this is an excellent assumption for inorganic fillers of bulk materials like zeolites or metal-organic frameworks, and also for flakes that contain a substantial number of layers, its validity is not clear for exfoliated flakes of nanoscopic thickness. Since it is not clear whether the small (~1 nm) thickness of the flake allows the establishment of a true random walk condition of the diffusing molecule, the definitions of diffusivity and permeability in such thin flakes are not physically obvious. Konduri and Nair constructed a molecular model of AMH-3 layers dispersed in a polydimethylsiloxane (PDMS) matrix and calculated the effective diffusivities of several gases through such composites (Konduri and Nair, 2007). It was found that the Cussler model greatly underpredicted the effective diffusivity. Similarly, experimental data on AMH-3/CA membranes could not be reconciled with the model predictions (solid line in Fig. 11b), even in the limit of the highest possible permeability predicted by the model (Kim et al., 2013). It has been suggested by the above authors that membranes containing nanoscopically thin flakes might be better modeled as nanoscale composite structures, and cannot be described by analytical models that assume bulk permeation behavior in the flakes.

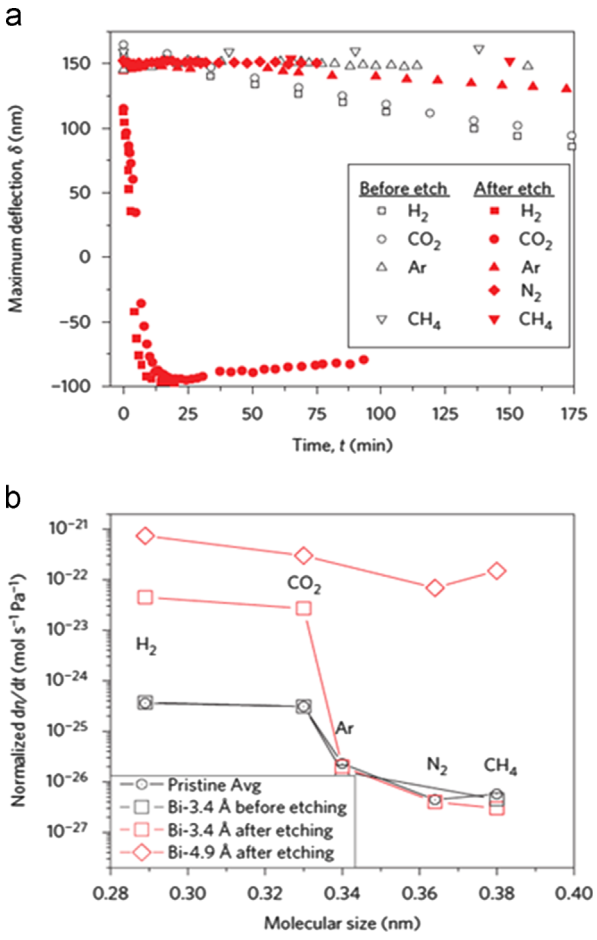

Fig. 12. Comparison of gas permeation rates of pristine and porous graphene membranes: (a) maximum deflection of the membrane surface versus time before and after etching, and (b) gas permeance versus molecular size, revealing selective permeation of H_2 and CO_2 over larger gas molecules after etching (adapted from Koenig et al., 2012).

4.3. Graphene and other carbon membranes

The first experimental evidence of gas separation by porous graphene was obtained *via* a 'pressurized blister' test with an atomically thin membrane (Koenig et al., 2012). Ultra-violet oxidative etching was used to introduce pores in a fabricated non-porous graphene membrane. The deformation of the film surface due to gas pressure on the feed side was measured to quantify the permeability, with a higher deflection indicating a lower permeability due to the gas molecules not being able to pass the graphene barrier. The etched porous graphene membrane was found to be selective (Fig. 12) for H_2 and CO_2 over larger molecules like Ar, N_2, and CH_4, hence suggesting the presence of pores slightly larger than 0.3 nm in size.

Nair et al. reported very rapid permeation of water through a 'leak-tight', non-porous multilayer graphene oxide membrane (Nair et al., 2012). The membrane was determined to be non-porous due to a very low He permeability in comparison to both a barrier polymer like PET (currently used as a commercial packaging material) as well as 1-mm-thick glass. However, the water permeability of the membrane was found to be extremely high (Fig. 13), and was described as 'unimpeded permeation of water'. This unusual property, observed to varying extents with molecules like water, ethanol, and hexane, could be explained by a nanoscale capillary effect whereby monolayers of water molecules form between graphene layers. This effect was also demonstrated by atomistic simulations.

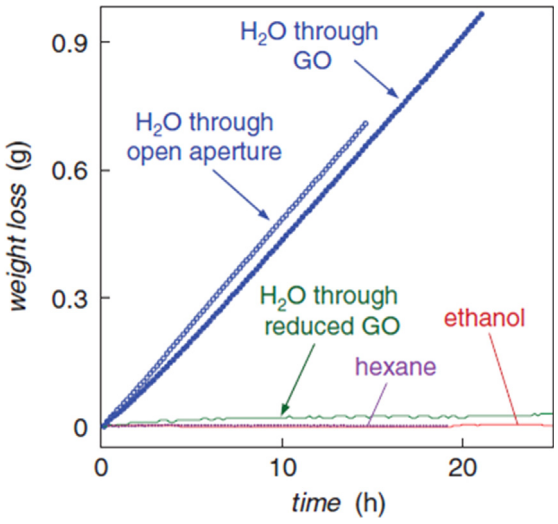

Fig. 13. Permeation of water, ethanol, and hexane through a graphene oxide membrane (adapted from Nair et al., 2012).

While graphene-based membranes are actively being developed, other carbon-based membranes have also shown potentially interesting properties. Diamond-like carbon (DLC) porous nanosheets (10–40 nm thin) have been recently fabricated by plasma chemical vapor deposition, and allowed ultrafast viscous permeation of organic solvents (Karan et al., 2012). The sub-nanometer pore size of the DLC membrane allowed selective organic solvent separation from larger solute molecules. While carbon molecular sieve (CMS) membranes produced by pyrolysis have been known for several decades and currently have more optimal transport properties than graphene and DLC membranes, they have some limitations such as a rather low permeability, and fragility especially in oxygen-containing environments (Ismail et al., 2011). The new developments on graphene and DLC membranes, while currently not as advanced as other 2D and 1D materials in fabricating functional and cost-effective membranes, may be promising future alternatives for applications in both gas and liquid separations. Different mechanisms for molecular separations in these membranes have been illustrated recently (Paul, 2012).

5. Outlook and challenges

Table 1 shows a (non-exhaustive) summary of the separation performance of membranes containing nanoporous 1D and 2D materials. It is seen that such membranes can perform highly selective separations in many industrially interesting applications, and that the permeation rates can be attractively high. In particular, Table 1 shows that membranes containing different nanoporous 1D and 2D materials are capable of separating a wide range

Table 1
Summary of separation performance of membranes utilizing 1D nanotubular and 2D nanoporous layered materials.

Membrane system	Separation	Permeability or permeance (of faster species)	Selectivity	1D or 2D material wt%
Gas-phase separations				
CNT/$BPPO_{dp}$ (Cong, 2007)	CO_2/N_2	150 Barrer	30	4–9
AlPO/Polyimide (Jeong et al., 2004)	CO_2/CH_4	28.3 Barrer	41	10
SAMH-3/PBI (Choi et al., 2008a, 2008b, 2008c)	H_2/CO_2	1.5 Barrer	30	2
SAMH-3/CA (Kim et al., 2013)	CO_2/CH_4	12 Barrer	30	2–6
JDF-L1/Copolyimide (Galve et al., 2011)	H_2/CH_4	150 Barrer	36	10
MCM-22 (Choi and Tsapatsis, 2010)	H_2/N_2	4×10^{-8} mol/m^2 s Pa	120	100
Exfoliated MWW (Varoon et al., 2011)	He/N_2	5×10^{-9} mol/m^2 s Pa	17	100
Porous graphene (Koenig et al., 2012)	CO_2/CH_4	1.5×10^{-12} mol/m^2 s Pa	10,000	100
Vapor-phase and pervaporative separations				
Aluminosilicate NT/PVA (Kang et al., 2012)	H_2O/EtOH	160,000 Barrer	35	40
Carbon NT/PVA (Choi et al., 2007)	H_2O/EtOH	1.1×10^{-8} mol/m^2 s Pa	49	5
Exfoliated Layered MFI (Varoon et al., 2011)	*p*-/*o*-xylene	3×10^{-7} mol/m^2 s Pa	70	100
Porous graphene oxide (Nair et al., 2012)	H_2O/He	1×10^{-6} Barrer	$> 10^{10}$	100
Membrane system	**Separation**	**H_2O flux**	**Salt rejection**	**1D material wt%**
Water separation				
CNT/polyamide (Chan et al., 2013)	H_2O/NaCl	28.7 gal/ft^2-day	98.6%	20
Membrane system	**Separation**	**H^+ conductivity**	**Selectivity (S-s/cm^3)**	**2D material wt%**
Selective proton conduction				
AMH-3/Nafion (Hudiono et al., 2009)	H^+/MeOH	4.2×10^{-2} S/cm	7.4×10^4	5
AMH-3 on Nafion (Kim et al., 2012)	H^+/MeOH	3.8×10^{-2} S/cm	2.2×10^4	100

of molecular species ranging from protons, small gas molecules, water, polar organic molecules, and larger nonpolar/hydrocarbon molecules (such as xylene isomers). The foregoing discussion has also shown that the transport mechanisms in these materials span not only the typical adsorption and diffusion phenomena seen in conventional nanoporous materials such as zeolites, but also reveal new features arising from the unique nanoscopic dimensions of the present 1D and 2D materials. Finally, the collection of materials discussed in this work already shows a wide spectrum of pore sizes (0.3–1 nm), which appears quite amenable to tailoring as well as range expansion *via* ongoing synthesis of new or modified 1D and 2D nanoporous materials.

Hence, it is reasonable to hypothesize that a large array of industrially attractive molecular separations can be targeted by membranes containing such materials. Because these materials can be synthesized or post-processed to obtain nanoscopic dimensions (*e.g.*, nanotubes as short as 10 nm, and layers/flakes as thin as 1 nm), they can be incorporated in very thin separating membrane layers (down to 100 nm or thinner), leading to higher throughput rates in comparison to more conventional porous membrane materials. As described in this review, a number of challenging synthesis and membrane processing issues have already been addressed *via* innovative materials synthesis chemistry and composite fabrication strategies. With the exception of the AlPO materials discussed briefly in Section 2.2, most of the 1D and 2D materials highlighted in this review show good stability and retention of their nanopore structures under processing conditions. These events, as well as the discovery of novel mechanisms of selective permeation in 1D and 2D materials such as carbon nanotubes and graphene, create an optimistic outlook that membranes containing 1D and 2D nanoporous materials may competitively address the many application opportunities available for next-generation separation technologies.

However, several challenges remain on the road to industrially scalable membranes incorporating nanoporous 1D and 2D materials. Effective strategies and platforms for membrane scale-up will be a critically important issue. Among the membrane types discussed in this review, those containing 2D layered materials can be considered as being furthest along the path to scale-up, since their processing strategies (as reviewed in this work) are seen to be compatible with polymeric membrane processing methods. For example, the incorporation of surface-modified nanoplatelets of the layered silicate laponite® into the skin layers of polyimide hollow fibers has been demonstrated (Johnson and Koros, 2009), thereby allowing the hypothesis that porous 2D materials can be processed in a similar manner into scalable membranes. However, it is yet unclear whether the techniques for inducing preferred orientation of 2D or 1D materials (as discussed earlier in this review) will also be compatible with membrane scale-up processes such as hollow fiber fabrication. In conjunction with the goal of membrane scale-up, there are two other important challenges. The first is regarding the scale-up of materials synthesis. Most of the materials described in this review have only been synthesized reproducibly in quantities of a few grams, a fact that prevents their testing in preliminary scale-up efforts such as hollow fiber membrane fabrication (which typically requires batches of ~100 g for a single experiment). However, due to the similarity of synthesis techniques of materials such as aluminosilicate nanotubes or layered zeolites in comparison to well-known zeolite materials that are in commercial uses, there is reason to believe that materials scale-up can be achieved in a similar manner to that of zeolites. The second challenge is to achieve a high uniformity of exfoliation and other processing steps. In their current state, exfoliation processes such as high-shear mixing or melt-blending of porous layered materials result in significantly polydisperse products containing well exfoliated flakes, partially exfoliated/intercalated flakes, and broken/damaged flakes or particles. Similarly, processing of nanotubes may lead to products containing a mixture of well dispersed nanotubes, aggregated bundles, and damaged nanotubes. Optimization of these processes will be required to produce high-quality exfoliated or dispersed 1D and 2D materials ready for membrane formation. The synthesis of pre-swollen or pre-exfoliated layered materials such as layered MFI, or well-dispersed aluminosilicate nanotubes in aqueous media, are initial examples described earlier in this review.

Another important challenge is the development of reliable structure-property relationships in these unique membrane systems (both by experimental characterization as well as by modeling and simulation), since they possess structural complexity over multiple length scales. At the nanoscopic level, there is now a diverse range of nanotubular and selective flake materials that have different pore structures, elemental compositions, and dimensions. There is currently little understanding of the mechanisms of selective separations by nanoporous 2D and 1D materials beyond the hypothesis of 'molecular sieving', based upon comparison of the nominal pore size of the material with the kinetic diameters of permeating molecules. Additionally, the question of finding a polymeric matrix transport properties that appropriately 'match' the nanoscopic materials and gives the highest overall composite membrane performance in a desired separation, remains unaddressed. Finally, the long-term stability characteristics of these nanocomposite membrane architectures have not yet been thoroughly evaluated, and very little data on this topic currently exists. Although recent examples of development of structure-property relations by experimental (e.g., SAXS/HRTEM/NMR) and computational (molecular modeling, finite-element simulations of microstructure) have appeared in the literature as discussed earlier in this review, significant work remains to be done to reach the stage of rationally designing or selecting nanoporous 1D and 2D materials for use in membrane separations.

Acknowledgment

This publication is based on work supported by Award no. KUS-I1-011-21, made by King Abdullah University of Science and Technology (KAUST).

References

Adams, R.T., et al., 2011. CO_2–CH_4 permeation in high zeolite 4A loading mixed matrix membranes. J. Membr. Sci. 367 (1–2), 197–203.
Allen, M.J., et al., 2010. Honeycomb carbon: A review of graphene. Chem. Rev. 110 (1), 132–145.
Bae, T.H., et al., 2009. Facile high-yield solvothermal deposition of inorganic nanostructures on zeolite crystals for mixed matrix membrane fabrication. J. Am. Chem. Soc. 131 (41), 14662–14663.
Bernardo, P., et al., 2009. Membrane gas separation: a review/state of the art. Ind. Eng. Chem. Res. 48 (10), 4638–4663.
Bieri, M., et al., 2009. Porous graphenes: two-dimensional polymer synthesis with atomic precision. Chem. Commun. 45, 6919–6921.
Blankenburg, S., et al., 2010. Porous graphene as an atmospheric nanofilter. Small 6 (20), 2266–2271.
Bottero, I., et al., 2011. Synthesis and characterization of hybrid organic/inorganic nanotubes of the imogolite type and their behaviour towards methane adsorption. Phys. Chem. Chem. Phys. 13 (2), 744–750.
Bunch, J.S., et al., 2007. Electromechanical resonators from graphene sheets. Science 315 (5811), 490–493.
Caro, J., Noack, M., 2008. Zeolite membranes – recent developments and progress. Microporous and Mesoporous Mater. 115 (3), 215–233.
Centi, G., Perathoner, S., 2008. Catalysis by layered materials: a review. Microporous and Mesoporous Mater. 107 (1-2), 3–15.
Chamberlain, T.W., et al., 2011. Reactions of the inner surface of carbon nanotubes and nanoprotrusion processes imaged at the atomic scale. Nat. Chem. 3 (9), 732–737.
Chan, W.-F., et al., 2013. Zwitterion functionalized carbon nanotube/polyamide nanocomposite membranes for water desalination. ACS Nano 7 (6), 5308–5319.

Chen, W., Tao, X., 2005. Self-organizing alignment of carbon nanotubes in thermoplastic polyurethane. Macromol. Rapid Commun. 26 (22), 1763–1767.
Cheung, C.L., et al., 2002. Diameter-controlled synthesis of carbon nanotubes. J. Phys. Chem. B 106 (10), 2429–2433.
Choi, J., et al., 2009a. Grain boundary defect elimination in a zeolite membrane by rapid thermal processing. Science 325 (5940), 590–593.
Choi, J., Tsapatsis, M., 2010. MCM-22/silica selective flake nanocomposite membranes for hydrogen separations. J. Am. Chem. Soc. 132 (2), 448–449.
Choi, J.H., et al., 2007. Modification of performances of various membranes using MWNTs as a modifier. Macromol. Symposia 249, 610–617.
Choi, M., et al., 2009b. Stable single-unit-cell nanosheets of zeolite MFI as active and long-lived catalysts. Nature 461, 246–249.
Choi, S., et al., 2008a. Layered silicates by swelling of AMH-3 and nanocomposite membranes. Angew. Chem.-Int. Edition 47 (3), 552–555.
Choi, S., et al., 2008b. Layered silicate by proton exchange and swelling of AMH-3. Microporous Mesoporous Mater. 115 (1-2), 75–84.
Choi, S.H., et al., 2008c. Fabrication and gas separation properties of polybenzimidazole (PBI)/nanoporous silicates hybrid membranes. J. Membr. Sci. 316 (1-2), 145–152.
Choudalakis, G., Gotsis, A., 2009. Permeability of polymer/clay nanocomposites: a review. Eur. Polym. J. 45 (4), 967–984.
Clavé, G., et al., 2013. Functionalization of carbon nanotubes through polymerization in micelles: a Bridge between the covalent and non-covalent methods. Chem. Mater. 25 (13), 2700–2707.
Cong, H.L., et al., 2007. Carbon nanotube composite membranes of brominated poly (2,6-diphenyl-1,4-phenylene oxide) for gas separation. J. Membr. Sci. 294 (1-2), 178–185.
Corma, A., et al., 2000. New aluminosilicate and titanosilicate delaminated materials active for acid catalysis, and oxidation reactions using H2O2. J. Am. Chem. Soc. 122 (12), 2804–2809.
Corma, A., et al., 2001. ITQ-18 a new delaminated stable zeolite. Chem. Commun. 24, 2642–2643.
Corma, A., et al., 1998. Delaminated zeolite precursors as selective acidic catalysts. Nature 396 (6709), 353–356.
Cussler, E.L., 1990. Membranes containing selective flakes. J. Membr. Sci. 52 (3), 275–288.
Dasgupta, S., Torok, B., 2008. Application of clay catalysts in organic synthesis. A review. Org. Prep. Proc. Int. 40 (1), 1–65.
Davis, M.E., 2002. Ordered porous materials for emerging applications. Nature 417 (6891), 813–821.
De Heer, W.A., et al., 1995. Aligned carbon nanotube films – production and optical and electronic-properties. Science 268 (5212), 845–847.
Diaz, I., et al., 2004. Surface structure of zeolite (MFI) crystals. Chem. Mater. 16 (25), 5226–5232.
Dyke, C.A., Tour, J.M., 2004. Covalent functionalization of single-walled carbon nanotubes for materials applications. J. Phys. Chem. A 108 (51), 11151–11159.
Fischbein, M.D., Drndic, M., 2008. Electron beam nanosculpting of suspended graphene sheets. Appl. Phys. Lett. 93 (11), 113107. (: art. #).
Galve, A., et al., 2011. Copolyimide mixed matrix membranes with oriented microporous titanosilicate JDF-L1 sheet particles. J. Membr. Sci. 370 (1–2), 131–140.
Gascon, J., et al., 2012. Practical approach to zeolitic membranes and coatings: state of the art, opportunities, barriers, and future perspectives. Chem. Mater. 24 (15), 2829–2844.
Gebel, G., Diat, O., 2005. Neutron and x-ray scattering: suitable tools for studying ionomer membranes. Fuel Cells 5 (2), 261–276.
Goh, P., et al., 2013. Carbon nanotubes for desalination: performance evaluation and current hurdles. Desalination 308, 2–14.
Gorgojo, P., et al., 2011. Direct exfoliation of layered zeolite Nu-6(1). Microporous Mesoporous Mater. 142 (1), 122–129.
Hanley, H.J.M., et al., 2003. A small-angle neutron scattering study of a commercial organoclay dispersion. Langmuir 19 (14), 5575–5580.
He, Y.J., et al., 1998. Synthesis, characterization and catalytic activity of the pillared molecular sieve MCM-36. Microporous Mesoporous Mater. 25 (1–3), 207–224.
Ho, D.L., et al., 2001. Characterization of organically modified clays using scattering and microscopy techniques. Chem. Mater. 13 (5), 1923–1931.
Hudiono, Y., et al., 2009. Porous layered oxide/Nafion® nanocomposite membranes for direct methanol fuel cell applications. Microporous Mesoporous Mater. 118 (1-3), 427–434.
Ismail, A., et al., 2009. Transport and separation properties of carbon nanotube-mixed matrix membrane. Sep. Purif. Technol. 70 (1), 12–26.
Ismail, A.F., et al., 2011. Carbon-Based Membranes for Separation Processes. Springer, New York.
Jagur-Grodzinski, J., 2007. Polymeric materials for fuel cells: concise review of recent studies. Polym. Adv. Technol. 18 (10), 785–799.
Jain, R., et al., 2010. Processing, structure, and properties of PAN/MWNT composite fibers. Macromol. Mater. Eng. 295 (8), 742–749.
Jeazet, H.B.T., et al., 2012. Metal–organic frameworks in mixed-matrix membranes for gas separation. Dalton Trans. 41 (46), 14003–14027.
Jeong, H.K., et al., 2004. Fabrication of polymer/selective-flake nanocomposite membranes and their use in gas separation. Chem. Mater. 16 (20), 3838–3845.
Jeong, H.K., et al., 2003. A highly crystalline layered silicate with three-dimensionally microporous layers. Nat. Mater. 2 (1), 53–58.
Jiang, D.E., et al., 2009. Porous graphene as the ultimate membrane for gas separation. Nano Lett. 9 (12), 4019–4024.
Johnson, J.R., Koros, W.J., 2009. Utilization of nanoplatelets in organic-inorganic hybrid separation materials: Separation advantages and formation challenges. J. Taiwan Inst. Chem. Eng. 40 (3), 268–275.
Jung, D.H., et al., 2003. Preparation and performance of a Nafion (R)/montmorillonite nanocomposite membrane for direct methanol fuel cell. J. Power Sour. 118 (1–2), 205–211.
Kang, D.-Y., et al., 2011a. Single-walled aluminosilicate nanotubes with organic-modified interiors. J. Phys. Chem. C 115 (15), 7676–7685.
Kang, D.Y., et al., 2011b. Modeling molecular transport in composite membranes with tubular fillers. J. Membr. Sci. 381 (1–2), 50–63.
Kang, D.Y., et al., 2012. Single-walled aluminosilicate nanotube/poly(vinyl alcohol) nanocomposite membranes. ACS Appl. Mater. Interfaces 4 (2), 965–976.
Karan, S., et al., 2012. Ultrafast viscous permeation of organic solvents through diamond-like carbon nanosheets. Science 335 (6067), 444–447.
Kim, J., et al., 2012a. Delamination of microporous layered silicate by acid-hydrothermal treatment and its use for reduction of methanol crossover in DMFC. Microporous Mesoporous Mater. 168, 148–154.
Kim, S., et al., 2007. Scalable fabrication of carbon nanotube/polymer nanocomposite membranes for high flux gas transport. Nano Lett. 7 (9), 2806–2811.
Kim, W.-G., et al., 2013. Nanoporous layered silicate AMH-3/cellulose acetate nanocomposite membranes for gas separations. J. Membr. Sci. 441, 129–136.
Kim, W., et al., 2012b. Epitaxially grown layered MFI-bulk MFI hybrid zeolitic materials. ACS Nano 6 (11), 9978–9988.
Kim, W.G., et al., 2011. Swelling, functionalization, and structural changes of the nanoporous layered silicates AMH-3 and MCM-22. Langmuir 27 (12), 7892–7901.
Kloprogge, J.T., 1998. Synthesis of smectites and porous pillared clay catalysts: a review. J. Porous Mater. 5 (1), 5–41.
Koenig, S.P., et al., 2012. Selective molecular sieving through porous graphene. Nature Nanotechnol. 7 (11), 728–732.
Konduri, S., Nair, S., 2007. A computational study of gas molecule transport in a polymer/nanoporous layered silicate nanocomposite membrane material. J. Phys. Chem. C 111 (5), 2017–2024.
Konduri, S., et al., 2008. Water in single-walled aluminosilicate nanotubes: diffusion and adsorption properties. J. Phys. Chem. C 112 (39), 15367–15374.
Koros, W.J., 2004. Evotving beyond the thermat age of separation processes: membranes can lead the way. AIChE J. 50 (10), 2326–2334.
Kratky, O., Porod, G., 1949. Diffuse small-angle scattering of X-rays in colloid systems. J. Colloid Sci. 4 (1), 35–70.
Krikorian, V., Pochan, D.J., 2003. Poly (L-lactic acid)/layered silicate nanocomposite: fabrication, characterization, and properties. Chem. Mater. 15 (22), 4317–4324.
Kulkarni, S., et al., 1994. Investigation of the pore structure and morphology of cellulose-acetate membranes using small-angle neutron-scattering. 2. Ultrafiltration and reverse-osmosis membranes. Macromolecules 27 (23), 6785–6790.
Lee, S.S., et al., 2005. Exfoliation of layered silicate facilitated by ring-opening reaction of cyclic oligomers in PET-clay nanocomposites. Polymer 46 (7), 2201–2210.
Leonowicz, M.E., et al., 1994. Mcm-22 – a molecular-sieve with 2 independent multidimensional channel systems. Science 264 (5167), 1910–1913.
Li, J.Y., et al., 1999. Structures and templating effect in the formation of 2D layered aluminophosphates with Al3P4O163-stoichiometry. Chem. Mater. 11 (9), 2600–2606.
Li, Y.F., et al., 2010. Two-dimensional polyphenylene: experimentally available porous graphene as a hydrogen purification membrane. Chem. Commun. 46 (21), 3672–3674.
Lin, Y.F., et al., 2007. A novel composite membranes based on sulfonated montmorillonite modified Nafion((R)) for DMFCs. J. Power Sources 168 (1), 162–166.
Liu, H.T., et al., 2009. Photochemical reactivity of graphene. J. Am. Chem. Soc. 131 (47), 17099–17100.
Liu, P., 2007. Polymer modified clay minerals: a review. Appl. Clay Sci. 38 (1–2), 64–76.
Mahajan, R., Koros, W.J., 2002. Mixed matrix membrane materials with glassy polymers. Part 1. Polym. Eng. Sci.42 (7), 1420–1431.
Majumder, M., et al., 2011. Mass transport through carbon nanotube membranes in three different regimes: ionic diffusion and gas and liquid flow. ACS Nano 5 (5), 3867–3877.
Matranga, C., et al., 2006. Raman spectroscopic investigation of gas interactions with an aligned multiwalled carbon nanotube membrane. Langmuir 22 (3), 1235–1240.
Mauter, M.S., et al., 2010. Nanocomposites of vertically aligned single-walled carbon nanotubes by magnetic alignment and polymerization of a lyotropic precursor. ACS Nano 4 (11), 6651–6658.
Merkel, T.C., et al., 2002. Ultrapermeable, reverse-selective nanocomposite membranes. Science 296 (5567), 519–522.
Messersmith, P.B., Giannelis, E.P., 1994. Synthesis and characterization of layered silicate-epoxy nanocomposites. Chem. Mater. 6 (10), 1719–1725.
Moermans, B., et al., 2000. Incorporation of nano-sized zeolites in membranes. Chem. Commun. 24, 2467–2468.
Mukherjee, S., et al., 2005. Phenomenology of the growth of single-walled aluminosilicate and aluminogermanate nanotubes of precise dimensions. Chem. Mater. 17 (20), 4900–4909.
Mukherjee, S., et al., 2007. Short, highly ordered, single-walled mixed-oxide nanotubes assemble from amorphous nanoparticles. J. Am. Chem. Soc. 129 (21), 6820–6826.
Na, K., et al., 2010. Pillared MFI zeolite nanosheets of a single-unit-cell thickness. J. Am. Chem. Soc. 132 (12), 4169–4177.
Nair, R.R., et al., 2012. Unimpeded permeation of water through helium-leak-tight graphene-based membranes. Science 335 (6067), 442–444.

Nasir, R., et al., 2013. Material advancements in fabrication of mixed-matrix membranes. Chem. Eng. & Technol. 36 (5), 717–727.

Novoselov, K.S., et al., 2004. Electric field effect in atomically thin carbon films. Science 306 (5696), 666–669.

Pandey, P., Chauhan, R.S., 2001. Membranes for gas separation. Prog. Polym. Sci. 26 (6), 853–893.

Park, J.Y., Paul, D.R., 1997. Correlation and prediction of gas permeability in glassy polymer membrane materials via a modified free volume based group contribution method. J. Membr. Sci. 125 (1), 23–39.

Paul, D.R., 2012. Creating new types of carbon-based membranes. Science 335 (6067), 413–414.

Paul, D.R., Robeson, L.M., 2008. Polymer nanotechnology: nanocomposites. Polymer 49 (15), 3187–3204.

Pavlidou, S., Papaspyrides, C.D., 2008. A review on polymer-layered silicate nanocomposites. Prog. Polym. Sci. 33 (12), 1119–1198.

Pendergast, M.M., Hoek, E.M., 2011. A review of water treatment membrane nanotechnologies. Energy Environ. Sci. 4 (6), 1946–1971.

Pinnau, I., He, Z.J., 2004. Pure- and mixed-gas permeation properties of polydimethylsiloxane for hydrocarbon/methane and hydrocarbon/hydrogen separation. J. Membr. Sci. 244 (1–2), 227–233.

Pinnavaia, T.J., 1983. Intercalated clay catalysts. Science 220 (4595), 365–371.

Prolongo, S.G., et al., 2013. In situ processing of epoxy composites reinforced with graphene nanoplatelets. Composites Sci. Technol. 86, 185–191.

Pujari, S., et al., 2009. Orientation dynamics in multiwalled carbon nanotube dispersions under shear flow. J. Chem. Phys.130 (21), 214903.

Rao, C.N.R., Govindaraj, A., 2009. Synthesis of inorganic nanotubes. Adv. Mater. 21 (42), 4208–4233.

Ray, S.S., Bousmina, M., 2005. Biodegradable polymers and their layered silicate nano composites: In greening the 21st century materials world. Prog. Mater. Sci. 50 (8), 962–1079.

Ray, S.S., Okamoto, M., 2003. Polymer/layered silicate nanocomposites: a review from preparation to processing. Prog. Polym. Sci. 28 (11), 1539–1641.

Rhee, C.H., et al., 2005. Nafion/sulfonated montmorillonite composite: a new concept electrolyte membrane for direct methanol fuel cells. Chem. Mater. 17 (7), 1691–1697.

Roberts, M.A., et al., 1996. Synthesis and structure of a layered titanosilicate catalyst with five-coordinate titanium. Nature 381, 401–404.

Robeson, L.M., 2008. The upper bound revisited. J. Membr. Sci. 320 (1-2), 390–400.

Roy, N., et al., 2012. Modifications of carbon for polymer composites and nanocomposites. Prog. Polym. Sci. 37 (6), 781–819.

Rubio, C., et al., 2010. Exfoliated titanosilicate material UZAR-S1 obtained from JDF-L1. Eur. J. Inorg. Chem., 159–163.

Schaefer, D.W., Justice, R.S., 2007. How nano are nanocomposites? Macromolecules 40 (24), 8501–8517.

Schmidt-Rohr, K., Chen, Q., 2008. Parallel cylindrical water nanochannels in nafion fuel-cell membranes. Nat. Mater. 7 (1), 75–83.

Schrier, J., 2010. Helium separation using porous graphene membranes. J. Phys. Chem. Lett. 1 (15), 2284–2287.

Schultz, J., Peinemann, K.V., 1996. Membranes for separation of higher hydrocarbons from methane. J. Membr. Sci. 110 (1), 37–45.

Shah, M., et al., 2012. Current status of metal–organic framework membranes for gas separations: promises and challenges. Ind. Eng. Chem. Res. 51 (5), 2179–2199.

Shao, Y.Y., et al., 2010. Graphene based electrochemical sensors and biosensors: a review. Electroanalysis 22 (10), 1027–1036.

Sheffel, J.A., Tsapatsis, M., 2007. A model for the performance of microporous mixed matrix membranes with oriented selective flakes. J. Membr. Sci. 295, 50–70.

Sheffel, J.A., Tsapatsis, M., 2009. A semi-empirical approach for predicting the performance of mixed matrix membranes containing selective flakes. J. Membr. Sci. 326, 595–607.

Shu, S., et al., 2007. A general strategy for adhesion enhancement in polymeric composites by formation of nanostructured particle surfaces. J. Phys. Chem. C 111 (2), 652–657.

Sieffert, D., Staudt, C., 2011. Preparation of hybrid materials containing copolyimides covalently linked with carbon nanotubes. Sep. Purif. Technol. 77 (1), 99–103.

Skoulidas, A.I., et al., 2002. Rapid transport of gases in carbon nanotubes. Phys. Rev. Lett. 89 (18), 185901.

Snyder, M.A., Tsapatsis, M., 2007. Hierarchical nanomanufacturing: from shaped zeolite nanoparticles to high-performance separation membranes. Angew. Chem.-Int. Edition 46 (40), 7560–7573.

Sokhan, V.P., et al., 2002. Fluid flow in nanopores: accurate boundary conditions for carbon nanotubes. J. Chem. Phys. 117 (18), 8531–8539.

Sokhan, V.P., et al., 2004. Transport properties of nitrogen in single walled carbon nanotubes. J. Chem. Phys. 120 (8), 3855–3863.

Staley, N., et al., 2007. Lithography-free fabrication of graphene devices. Appl. Phys. Lett. 90, 14.

Stern, S.A., et al., 1989. Structure permeability relationships of polyimide membranes – applications to the separation of gas-mixtures. J. Polym. Sci. Part B-Polym. Phys. 27 (9), 1887–1909.

Tenne, R., Seifert, G., 2009. Recent progress in the study of inorganic nanotubes and fullerene-like structures. Ann. Rev. Mater. Res. 39, 387–413.

Thill, A., et al., 2012a. How the diameter and structure of (OH) $3Al_2O_3SixGe1–xOH$ imogolite nanotubes are controlled by an adhesion versus curvature competition. J. Phys. Chem. C 116 (51), 26841–26849.

Thill, A., et al., 2012b. Physico-chemical control over the single-or double-wall structure of aluminogermanate imogolite-like nanotubes. J. Am. Chem. Soc. 134 (8), 3780–3786.

Thomas, J.M., et al., 2001. Molecular sieve catalysts for the regioselective and shape-selective oxyfunctionalization of alkanes in air. Acc. Chem. Res. 34 (3), 191–200.

Thomassin, J.M., et al., 2006. Improvement of the barrier properties of nafion (R) by fluoro-modified montmorillonite. Solid State Ionics 177 (13–14), 1137–1144.

Tkalya, E.E., et al., 2012. The use of surfactants for dispersing carbon nanotubes and graphene to make conductive nanocomposites. Curr. Opin. Colloid Interface Sci. 17 (4), 225–232.

Tung, V.C., et al., 2009. High-throughput solution processing of large-scale graphene. Nat. Nanotechnol. 4 (1), 25–29.

Urban, K.W., 2011. Electron microscopy: the challenges of graphene. Nat. Mater. 10 (3), 165–166.

Usuki, A., et al., 1993. Synthesis of nylon 6-clay hybrid. J. Mater. Res. 8 (5), 1179–1184.

Vaia, R.A., Maguire, J.F., 2007. Polymer nanocomposites with prescribed morphology: going beyond nanoparticle-filled polymers. Chem. Mater. 19 (11), 2736–2751.

Vaisman, L., et al., 2006. The role of surfactants in dispersion of carbon nanotubes. Adv. Colloid Interface Sci. 128, 37–46.

Vane, L.M., 2005. A review of pervaporation for product recovery from biomass fermentation processes. J. Chem. Technol. Biotechnol. 80 (6), 603–629.

Vane, L.M., et al., 2008. Hydrophobic zeolite-silicone rubber mixed matrix membranes for ethanol–water separation: effect of zeolite and silicone component selection on pervaporation performance. J. Membr. Sci. 308 (1-2), 230–241.

Varoon, K., et al., 2011. Dispersible exfoliated zeolite nanosheets and their application as a selective membrane. Science 333 (6052), 72–75.

Vinh-Thang, H., Kaliaguine, S., 2013. Predictive models for mixed-matrix membrane performance: a review. Chem. Rev. 113 (7), 4980–5028.

Vu, D.Q., et al., 2003. Mixed matrix membranes using carbon molecular sieves – I. preparation and experimental results. J. Membr. Sci. 211 (2), 311–334.

Wang, B.N., et al., 2007. Characterizing the morphologies of mechanically manipulated multiwall carbon nanotube films by small-angle X-ray scattering. J. Phys. Chem. C 111 (48), 17933–17940.

Williams, I.D., et al., 1996. Organo-template control of inorganic structures: a low-symmetry two-dimensional sheet aluminophosphate $3[NH_3CHMeCH_2NH_3][Al_6P_8O_{32}]$. H_2O. Chem. Commun. 15, 1781–1782.

Williams, I.D., et al., 1997. New chain architecture for a one-dimensional aluminophosphate, $[H_3NCH_2CH_2NH_3][AlP_2O_8H]$. Chem. Commun. 14, 1273–1274.

Xu, B., et al., 2009. Evolution of clay morphology in polypropylene/montmorillonite nanocomposites upon equibiaxial stretching: a solid-state NMR and TEM approach. Macromolecules 42 (22), 8959–8968.

Yan, W.F., et al., 2000. A novel open-framework aluminophosphate $[AlP_2O_6(OH)_2][H_2O]$ containing propeller-like chiral motifs. Chem. Commun. 15, 1431–1432.

Yoonessi, M., et al., 2005. Clay delamination in clay/poly(dicyclopentadiene) nanocomposites quantified by small angle neutron scattering and high-resolution transmission electron microscopy. Macromolecules 38 (3), 818–831.

Yu, J., et al., 1998a. $Al_{16}P_{20}O_{80}H_4.4C_6H_{18}N_2$: A new microporous aluminophosphate containing intersecting 12- and 8-membered ring channels. Chem. Mater. 10 (5), 1208–1211.

Yu, J., et al., 1998b. Solvothermal synthesis and characterization of new aluminophosphate layers templated by imidazolium ions. Supramol. Sci. 5 (3–4), 297–302.

Yucelen, G.I., et al., 2011. Formation of single-walled aluminosilicate nanotubes from molecular precursors and curved nanoscale intermediates. J. Am. Chem. Soc. 133 (14), 5397–5412.

Yucelen, G.I., et al., 2012. Shaping single-walled metal oxide nanotubes from precursors of controlled curvature. Nano Lett. 12 (2), 827–832.

Zang, J., et al., 2010. Flexibility of ordered surface hydroxyls influences the adsorption of molecules in single-walled aluminosilicate nanotubes. J. Phys. Chem. Lett. 1 (8), 1235–1240.

Zang, J., et al., 2009. Self-diffusion of water and simple alcohols in single-walled aluminosilicate nanotubes. ACS Nano 3 (6), 1548–1556.

Zhao, Y.-L., Stoddart, J.F., 2009. Noncovalent functionalization of single-walled carbon nanotubes. Accounts Chem. Res. 42 (8), 1161–1171.

Zornoza, B., et al., 2011. Mixed matrix membranes for gas separation with special nanoporous fillers. Desalination Water Treat. 27 (1–3), 42–47.